Running title: Scattering and Attenuation

Chapter 11. Scattering and Attenuation of Seismic Waves in the Lithosphere

Haruo Sato*, Mike Fehler** and Ru-Shan Wu***
*Dept. of Geophysics, Science, Tohoku University, Sendai, Japan,
**Los Alamos National Laboratory, Los Alamos, New Mexico, USA,
***Institute of Tectonics, University of California, Santa Cruz, California, USA.

Abstract

This chapter covers recent developments in observational and theoretical studies on scattering and attenuation of high-frequency seismic waves in the earth's lithosphere. There are two distinct physical mechanisms for attenuation, intrinsic absorption and scattering loss due to distributed heterogeneities. The most prominent evidence for the existence of small-scale random heterogeneities is the existence of "coda" which is the tail portion of the seismograms of local earthquakes. The radiative transfer theory is introduced to account for the effects of multiple scattering and provides an efficient way to model observed coda characteristics of local earthquakes. The coda normalization method is widely used for the estimation of site amplification factors, source spectra, and attenuation per travel distance. There is also a stochastic method to invert for the spectral structure of the random heterogeneity from the coherence analysis of seismic array data. This method focuses on forward scattering characteristics. For forward modeling, there are various approaches for numerically calculating wave propagation in heterogeneous media.

Glossaries: Born approximation, coda waves, coda attenuation, coda normalization method, coherence, duration magnitude, ensemble of random

media, envelope broadening, lapse time, parabolic approximation, Q value, radiative transfer theory, random media, Rytov method, scattering, scattering coefficient, seismic albedo, seismic array.

I. Attenuation of seismic waves

Scattering and attenuation of high-frequency seismic waves are important parameters to quantify and to physically characterize the earth medium. We first compile measurements of attenuation of seismic waves, and discuss physical mechanisms of attenuation in the lithosphere: intrinsic absorption and scattering loss due to distributed heterogeneities. As a model of attenuation, we introduce an approach for calculating the amount of scattering loss in a manner consistent with conventional seismological attenuation measurements.

A. Attenuation of P- and S-waves observed

The observed seismic-wave amplitudes usually decay exponentially with increasing travel distance after the correction for geometrical spreading, and decay rates are proportional to Q^{-1} which characterizes the attenuation. For spherically outgoing S-waves of frequency f in a uniform velocity structure, the spectral amplitude at a travel distance r goes roughly as $u^{\mathrm{S\,Direct}}(r;f) \propto e^{-\pi r f Q_S^{-1}/\beta_0}/r$, where β_0 is the S-wave velocity. We first compile reported values of Q_S^{-1} and Q_P^{-1} for the lithosphere in Figs. 1a and b, respectively. Anderson and Hart (1978) proposed $Q_S^{-1} \approx 0.002$, $Q_P^{-1} \approx 0.0009$, and ratio $Q_P^{-1}/Q_S^{-1} \approx 0.5$ for frequencies < 0.05 Hz for depths < 45 km. Analyzing teleseismic P- and S-waves, Taylor *et al.* (1986) found that Q_S^{-1} was larger in the Basin and Range Province than in the Shield. Analyzing records of microearthquakes in Kanto, Japan using the coda normalization method (see II D), Aki (1980) found that Q_S^{-1} decreases with increasing frequency as a power law $Q_S^{-1} \propto f^{-(0.6-0.8)}$ for 1–25 Hz. Kinoshita (1994) reported a decrease in Q_S^{-1}

with decreasing frequency for frequencies less than about 0.8 Hz (curve 16 in Fig. 1a) in southern Kanto, Japan. Yoshimoto *et al.* (1993) estimated $Q_S^{-1} \approx 0.012 f^{-0.73}$ and $Q_P^{-1} \approx 0.031 f^{-0.5}$ for 1–32 Hz in Kanto, Japan for depth < 100 km and the resultant ratio Q_P^{-1}/Q_S^{-1} is larger than 1. Yoshimoto *et al.* (1998) found rather strong attenuation in the shallow crust, $Q_S^{-1} \approx 0.0034 f^{-0.12}$ and $Q_P^{-1} \approx 0.052 f^{-0.66}$ for 25–102 Hz. Carpenter and Sanford (1985) reported $Q_P^{-1}/Q_S^{-1} \approx 1.5$ for 3–30 Hz in the upper crust of the central Rio Grande Rift.

We may summarize the observed characteristics as follows: Q_S^{-1} is of the order of 10^{-2} at 1 Hz and decreases to the order of 10^{-3} at 20 Hz. It seems reasonable to write the frequency dependence of attenuation in the form of a power law as $Q_S^{-1} \propto f^{-n}$ for frequencies higher than 1 Hz, where the power n ranges from 0.5 to 1. The frequency dependence at 0.1~1 Hz remains poorly understood because seismic measurements in this band are difficult to make. Results in Fig. 1b show that Q_P^{-1} also decreases with increasing frequency for frequencies higher than 1 Hz. For frequencies lower than 0.05 Hz, the ratio Q_P^{-1}/Q_S^{-1} has been taken to be a constant less than 1. Many have assumed that the ratio for higher frequencies is the same as for low frequencies. However, recent observations have clearly shown that the ratio Q_P^{-1}/Q_S^{-1} ranges between 1 and 2 for frequencies higher than 1 Hz. (Yoshimoto *et al.*, 1993).

There have been many attempts to derive attenuation tomogram images from the spectral decay analysis of recorded body waves (Clawson *et al*., 1989; Scherbaum and Wyss, 1990; Al-Shukri and Mitchell, 1990; Ponko and Sanders, 1994). It is important to overcome the trade-off between the frequency dependencies of source spectra and Q^{-1} and remove site amplification factors near the recording station for imaging the attenuation tomogram: some supposed the ω^2 model for source spectra and frequency independent Q^{-1} in the analyses.

Seismic attenuation is usually considered to be a combination of two mechanisms, scattering loss and intrinsic absorption. Measurements of attenuation

of direct seismic waves give values for total attenuation. Scattering redistributes wave energy within the medium. Conversely, intrinsic absorption refers to the conversion of vibration energy into heat. Wu (1985) introduced the concept of seismic albedo B_0 as the ratio of scattering loss to total attenuation.

B. Intrinsic absorption

There are several review papers that discuss proposed mechanisms for intrinsic absorption that lead to frequency-independent Q_P^{-1} and Q_S^{-1} (Knopoff, 1964; Jackson and Anderson, 1970; Mavko *et al.*, 1979; Dziewonski, 1979). For seismic waves to remain causal in the presence of attenuation, the relationship between frequency-dependent Q^{-1} and velocity dispersion was discussed by Liu *et al.* (1976).

Many proposed mechanisms are based on the observation that crustal rocks have microscopic cracks and pores which may contain fluids. These features have dimensions much smaller than the wavelengths of regional seismic phases. Walsh (1966) proposed frictional sliding on dry surfaces of thin cracks as an attenuation mechanism. Nur (1971) proposed viscous dissipation in a zone of partially molten rock to explain the low velocity/high attenuation zone beneath the lithosphere. Even though the addition of water reduces the melting temperature of rocks, it is unlikely that melted rock exists in most regions of the lithosphere. Mavko and Nur (1979) examined the effect of partial saturation of cracks on absorption: fluid movement within cracks is enhanced by the presence of gas bubbles. O'Connell and Budiansky (1977) proposed a model in which fluid moves between closely spaced adjacent cracks. Tittmann *et al.* (1980) measured an increase of Q_S^{-1} with increasing content of volatile in dry rocks. They found that the rapid increase was due to an interaction between adsorbed water film on the solid surface by thermally activated motions. Thermally activated processes at grain boundaries have been proposed as an absorption mechanism for the upper

mantle (Anderson and Hart, 1978; Lundquist and Cormier, 1980). Spatial temperature differences induced by adiabatic compression during wave propagation will be reduced by thermal diffusion (Zener, 1948; Savage, 1966a), which removes vibrational energy from the wave field. Grain-sized heterogeneities in a rock increase the amount of predicted absorption by this mechanism, which is called thermoelastic effect. Savage (1966b) investigated thermoelasticity caused by stress concentrations induced by the presence of cracks. Most of the mechanisms discussed above can predict Q_S^{-1} having values in the range of 10^{-3}; however, the importance of various mechanisms varies with depth, temperature, fracture content, fracture aspect ratios, pressure, and the presence of fluids. Aki (1980) discussed a relation between physical dimensions and the observed and partially conjectured frequency-dependence of Q_S^{-1} having a peak on the order of 0.01 around 0.5 Hz. He preferred thermoelasticity as the most viable model at lithospheric temperatures since the required scales for rock grains and cracks along with the amount of attenuation are in closest agreement with observations.

C. Scattering loss

Scattering due to heterogeneities distributed in the earth also causes a decrease in amplitude with travel distance (Aki, 1980), where the characteristic frequency is determined by a characteristic spatial scale, such as the correlation length of random media or the crack length. We begin to study scattering using the scalar-wave equation in inhomogeneous media. We suppose the wave velocity is written as $V(\mathbf{x}) = V_0\,[1 + \xi(\mathbf{x})]$, where V_0 is the background velocity and small fractional fluctuation $\xi(\mathbf{x})$ is a homogeneous and isotropic random function of coordinate $\mathbf{x}$. We imagine an ensemble of random media $\{\xi(\mathbf{x})\}$. First, we define the autocorrelation function (ACF) $R(\mathbf{x}) \equiv \langle \xi(\mathbf{y})\xi(\mathbf{y}+\mathbf{x}) \rangle$ as a statistical measure. The spatial scale and the strength of inhomogeneity are characterized by

correlation length a and the mean square fractional fluctuation ε^2, respectively. We divide the random medium into blocks of a dimension larger than a. We imagine a scalar plane-wave of angular frequency ω of unit amplitude incident upon a localized inhomogeneity. We calculate the generation of outgoing scattered waves using the Born approximation. Taking the ensemble average of scattering amplitude at scattering angle ψ, we get the differential scattering coefficient, which is the scattering power per unit volume, at angular frequency ω as

$$g(\psi;\omega) = \frac{k^4}{\pi} P\left(2k \sin\frac{\psi}{2}\right) \tag{1}$$

where wavenumber $k = \omega / V_0$ and P is the power spectral density function (PSDF) of random inhomogeneity. The fractional scattering loss of incident-wave energy per unit travel distance is the average of g over solid angle, which is total scattering coefficient g_0 (Aki and Richards, 1980). Dividing g_0 by k, we get scattering loss

$${}^{BSc}Q^{-1}(\omega) \equiv \frac{g_0}{k} = \frac{1}{4\pi k}\oint g(\psi;\omega) 2\pi \sin\psi d\psi = \frac{k^3}{2\pi}\int_0^{\pi} P\left(2k \sin\frac{\psi}{2}\right)\sin\psi d\psi \tag{2}$$

In the case of exponential ACF $R(\mathbf{x}) = \varepsilon^2 e^{-r/a}$, with PSDF $P(\mathbf{m}) = 8\pi\varepsilon^2 a^3 \Big/ \left(1 + a^2 m^2\right)^2$, the asymptotic behavior is ${}^{BSc}Q^{-1} \approx 2\varepsilon^2 ak$ for $ak >> 1$. As plotted by a dotted curve in Fig. 2, Eq. (2) predicts attenuation larger than ε^2 for large ak even if ε^2 is small. The large scattering loss here predicted for high frequencies is caused by strong forward scattering in a cone around the forward direction, $\psi < 1/ak$. There is a disagreement between ${}^{BSc}Q^{-1}$ obtained from direct application of the Born approximation and observed Q_S^{-1} which decreases with increasing frequency for high frequencies (see Fig. 1a). Wu (1982) proposed a method to calculate the scattering loss by specifying a lower bound of scattering angle $\psi_C = 90^\circ$ in Eq. (2) by arguing that this accounts only for the back-scattered energy, which is lost:

$$ {}^{Csc}Q^{-1}(\omega) = \frac{k^3}{2\pi} \int_{\psi_C}^{\pi} P\left(2k \sin\frac{\psi}{2}\right) \sin\psi \, d\psi \qquad (3) $$

Sato (1982) suggested that the strong increase in attenuation for high frequencies is due to the travel-time (phase) fluctuation caused by velocity fluctuation. He proposed a method to calculate the scattering loss after subtracting the travel-time fluctuation caused by velocity fluctuation of which the wavelengths are larger than twice the wavelength of incident waves, which corresponds to $\psi_C \approx 29^\circ$ in (3). For an exponential ACF, corrected scattering loss ${}^{Csc}Q^{-1}$ has a peak of the order of ε^2 at $ak \approx 1$, and becomes ${}^{Csc}Q^{-1}(\omega) \propto \varepsilon^2 / ak$ for $ak >> 1$. Solid curves in Fig. 2 show the scattering loss given by (3) against ak. Such a frequency dependence well explains the observed frequency dependence of attenuation as shown in Fig. 1. Extending the above idea to elastic vector-waves and fitting the predicted scattering loss curve to observed Q_S^{-1}, Sato (1984) estimated ε^2=0.01 and a=2 km for the lithosphere. The choice of ψ_C was numerically examined by several investigators (Frankel and Clayton, 1986; Roth and Korn, 1993; Fang and Müller, 1996).

There have been many studies of scattering by distributed cracks and cavities (Varadan *et al.*, 1978; Benites *et al.*, 1992; Benites *et al.*, 1997; Kikuchi, 1981; Matsunami, 1990; Kawahara and Yamashita, 1992). Scattering by cracks gives a peak in Q^{-1} when the wavelength is of the same order as the dimension of the crack; however, it is difficult to imagine open cracks having dimensions large enough to be comparable to regional seismic wavelengths deep in the earth.

II. Seismogram envelopes of local earthquakes

The appearance of coda waves in seismograms is one of the most prominent observations supporting the existence of small-scale random heterogeneities in the earth (Aki, 1969). We will now discuss characteristics of observed coda. Then we will introduce the radiative transfer theory, which can account for the effects of multiple scattering and model observed coda

characteristics. We compile measurements of total scattering coefficient and coda attenuation, which characterize coda excitation and coda amplitude decay, respectively. We will then discuss the coda normalization method, which is widely used for the estimation of attenuation per travel distance, site amplification factors, and source spectra on the basis of the spatially uniform distribution of coda energy at a long lapse time. Finally, we will present the multiple lapse time window analysis method that has been developed for the measurement of scattering loss and intrinsic absorption based on the solution of the radiative transfer theory.

A. Coda characteristics

We show seismograms of a typical local earthquake in Fig. 3: the direct S-wave is followed by complex wave trains, which are called “S-coda” or simply “coda”. Clear S-coda waves have been identified on seismograms recorded at the bottom of deep boreholes (Sato, 1978; Leary and Abercrombie, 1994). The *f-k* analysis of array seismic data shows that S-coda is composed of many wavelets arriving from various directions. Recorded waveforms show a large variation in amplitude near the direct S-arrival: however, the variation decreases as lapse time increases. S-coda waves have a common envelope shape at most stations near the epicenter after about twice the S-wave travel-time (Rautian and Khalturin, 1978). The logarithm of the trace duration of a local seismogram is generally proportional to earthquake magnitude. Trace duration has been used for the quick determination of earthquake magnitudes in many regions of the world (Tsumura, 1967).

B. Radiative Transfer Theory

Wu (1985) and Shang and Gao (1988) first introduced the radiative transfer theory into seismology, then Zeng *et al.* (1991) formulated the time-

dependent multiple scattering process in 3D. Here, we introduce a theory for multiple isotropic scattering process for a point shear-dislocation source (Sato *et al.*, 1997). We imagine a nonabsorbing 3D scattering medium with the background propagation velocity V_0, in which point-like isotropic scatterers of cross-section σ_0 are randomly and homogeneously distributed with density n, where $g_0 \equiv n\sigma_0$. We assume an impulsive source located at the origin of energy W with radiation pattern $\Xi(\theta,\phi)$ (see Fig. 4a) at time zero. The scattering process is written by

$$E(\mathbf{x},t) = W\Xi(\theta,\phi)G_E(\mathbf{x},t) + g_0 V_0 \int_{-\infty}^{\infty}\int_{-\infty}^{\infty}\int_{-\infty}^{\infty}\int_{-\infty}^{\infty} G_E(\mathbf{x}-\mathbf{x}',t-t')E(\mathbf{x}',t')d\mathbf{x}'\,dt' \tag{4}$$

where the convolution integral means the propagation of energy from the last scattering point to the receiver. The first term is for the direct propagation, where

$$G_E(\mathbf{x},t) = \frac{1}{4\pi V_0\, r^2} H(t)\delta\left(t-\frac{r}{V_0}\right)e^{-g_0 V_0 t} \tag{5}$$

We can analytically solve Eqs. (4)~(5) by using the Fourier-Laplace transform in space-time, and a spherical harmonics expansion in angle. For the case of spherical source radiation $\Xi = 1$, Zeng *et al.* (1991) got

$$\begin{aligned} E(\mathbf{x},t) = {} & \frac{W}{4\pi V_0 r^2}\delta\left(t-\frac{r}{V_0}\right)e^{-g_0 V_0 t}H(t) + \frac{Wg_0 e^{-g_0 V_0 t}}{4\pi r^2}\frac{r}{V_0 t}\ln\left[\frac{r+V_0 t}{r-V_0 t}\right]H\left(t-\frac{r}{V_0}\right) \\ & + Wg_0{}^2 V_0{}^2 \frac{1}{(2\pi)^2}\int_{-\infty}^{\infty}\int_{-\infty}^{\infty} d\omega dk\, e^{-i\omega t - ikr}\frac{ik}{2\pi r}\frac{\overline{\overline{G}}_{E0}(-k,-i\omega)^3}{1-g_0 V_0 \overline{\overline{G}}_{E0}(-k,-i\omega)} \end{aligned} \tag{6}$$

where $\overline{\overline{G}}_{E0}(k,s) = (1/kV_0)\tan^{-1} kV_0/(s+g_0 V_0)$. The second term shows the single scattering term (Sato, 1977; Kopnichev, 1975), which decreases according to the inverse square of lapse time at large lapse time as $Wg_0/2\pi V_0{}^2 t^2$ (Aki and Chouet, 1975).

We show temporal variations of normalized energy density ($\overline{E} = E/Wg_0{}^3$) against normalized lapse time ($\bar{t} = g_0 V_0 t$), at distance of one mean free path $r = g_0{}^{-1}$ for a point shear-dislocation source by solid curves (Sato *et al.*, 1997) in Fig. 4b. The energy density faithfully reflects the source radiation pattern near the direct arrival; however, the azimuthal dependence diminishes with increasing

lapse time. Each solid curve asymptotically converges to a broken curve for spherical source radiation. This simulation qualitatively agrees with the observed radiation pattern independence of coda amplitudes at long lapse time.

It should be mentioned that the energy flux model (Frankel and Wennerberg, 1987) and the use of Monte-Carlo methods (Hoshiba, 1991; Gusev and Abubakirov, 1996) for envelope synthesis played important roles in the coda study.

C. Coda attenuation and scattering coefficient

The coda energy density in a frequency band having central frequency f is a sum of the density times average square of particle-velocity of S coda around lapse time t, $u_i^{S\,\mathrm{Coda}}(t;f)$ as $E^{S\,\mathrm{Coda}}(t;f) \approx \sum_{i=1}^{3} \rho_0 u_i^{S\,\mathrm{Coda}}(t;f)^2$, where ρ_0 is the mass density. For practical analysis, we need to introduce an empirical parameter, known as coda attenuation Q_C^{-1}. In the case of single scattering model, the coda decay curve is given by

$$E^{S\,\mathrm{Coda}}(t;f) \approx \frac{W g_0}{2\pi V_0^2 t^2} e^{-Q_C^{-1}(f)\,2\pi f t} \quad \text{for} \quad t >> 2r/V_0 \qquad (7)$$

Fig. 5a summarizes reported coda attenuation. In general, Q_C^{-1} is about 10^{-2} at 1 Hz and decreases to about 10^{-3} at 20 Hz. The frequency dependence within a region can be written as $Q_C^{-1} \propto f^{-n}$ for f > 1 Hz, where n = 0.5 ~ 1. Regional differences of Q_C^{-1} were extensively studied in relation with seismotectonic settings (Singh and Herrmann, 1983; Matsumoto and Hasegawa, 1989; Jin and Aki, 1988). We may say that Q_C^{-1} is smaller in tectonically stable areas and larger in active areas. Comparing the observed coda energy density with that predicted from theoretical coda models, we can estimate total scattering coefficient g_0 for S-to-S scattering. Fig. 5b shows reported g_0, which is of the order of 10^{-2} km^{-1} for frequencies 1–30Hz, and each measurement has an error of about factor 2. Nishigami (1991) and later Revenaough (1995) inverted for the

spatial distribution of scattering coefficient from the analysis of S- and P-coda amplitude residuals from the average coda decay. There have been various attempts to map coda attenuation in various scales (O'Doherty *et al.*, 1997; Mitchell *et al*., 1997).

Seismic coda monitoring could provide information about the temporal change in fractures and attenuation caused by changes in tectonic stress during the earthquake cycle (Chouet, 1979). Jin and Aki (1986) reported a change in Q_C^{-1} associated with the occurrence of the Tangshan earthquake. Fehler *et al.* (1988) found differences in Q_C^{-1} before and after an eruption of Mt. St. Helens volcano. There have been many studies that indicate a correlation between temporal change in coda characteristics and the occurrence of large earthquakes. However, there have been criticisms such as about the possible influences of using different lapse times to establish the temporal change in coda characteristics and the effects of differing focal mechanisms and earthquake locations (Sato, 1988; Frankel, 1991; Ellsworth, 1991). Got *et al.* (1990) proposed to use earthquake doublets. Recent measurements try to reflect those criticisms (Aster *et al.*, 1996). Analyzing short-period seismograms recorded at Riverside, California between 1933 to 1987, Jin and Aki (1989) reported a temporal variability in Q_C^{-1} and a positive correlation with the seismic b-value. Gusev (1995) summarized coda observations made between 1967 and 1992 in Kamchatka by plotting coda magnitude residuals, and he reported two prominent anomalies.

D. Coda Normalization method

Coda waves provide a reliable way to isolate and quantify seismic propagation effects. Based on the single scattering model, we may write the average coda amplitude at a long lapse time t_c from the origin time at central frequency *f* as a product of the source, propagation and site amplification as $u^{S\text{-Coda}}(t_c;f) \propto \sqrt{g_0(f)W_i^S(f)}\,N_j^S(f)\,e^{-Q_C^{-1}\pi f t_c}/t_c$, where $N_j^S(f)$ is the site

amplification factor, $W_i^S(f)$ is the S-wave source energy. We suppose that $g_0(f)$ is constant. The direct S-wave amplitude is written as $u_{ij}^{S\,\mathrm{Direct}}(r;f) \propto \sqrt{W_i^S(f)}N_j^S(f)e^{-Q_S^{-1}\pi f r/\beta_0}/r$, where r is the hypocentral distance. Aki (1980) proposed a correction for source size and site amplification by normalizing direct S-wave amplitude by S-coda amplitude. Taking the logarithm of the ratio of the product of r and the direct S-wave amplitude to the averaged coda amplitude, where the common site amplification and source terms cancel, we get

$$\ln\left[r u_{ij}^{S\,\mathrm{Direct}}(r;f)/u_{ij}^{S\,\mathrm{Coda}}(t_c;f)\right] = -\left(Q_S^{-1}(f)\pi f/\beta_0\right)r + \mathrm{Const.} \qquad (8)$$

We may smooth out the radiation pattern differences when the measurements are made over a large enough number of earthquakes. Plotting the LHS of (8) against *r*, the gradient gives the attenuation per travel distance. Aki (1980) first used this method for the estimation of Q_S^{-1} in Japan. Later, Yoshimoto *et al.* (1993) extended this method to measure Q_P^{-1}.

The ratio of coda amplitudes at different sites gives the relative site amplification factor since the source factor is common. Tsujiura (1978) found that estimates of site effects made using coda are similar to those obtained from direct wave measurements. He also found less variability in site effect measurements made for a single site using coda waves from various sources than from direct waves for the same sources. The ratio of coda amplitudes of difference earthquakes at a single station gives the relative source radiation since the site factor is common. These methods have been widely used in the world (Biswas and Aki, 1984; Phillips and Aki, 1986; Dewberry and Crosson, 1995; Hartse *et al.*, 1995).

E. Multiple lapse-time window analysis

For the determination of seismic albedo B_0, Fehler *et al.* (1992) and Hoshiba *et al.* (1991) developed a method based on two observations: the early portion of an S-wave seismogram is dominated by the direct S-wave whose

amplitude change with distance is controlled by the total attenuation of the media; and S-coda level is composed entirely of scattered S-waves whose amplitudes are controlled by the total scattering coefficient. Their method is based on the radiative transfer theory, in which scattering is assumed to be isotropic and radiation is spherically symmetric. They evaluate the integrated energy density as a function of source-receiver distance and medium parameters. Fehler *et al.* (1992) analyzed seismograms of local earthquakes in Kanto–Tokai, Japan in three frequency bands. Fig. 6 shows the energy density integrated over three time-windows for 4–8 Hz band. The running means of the data over 15 km windows is plotted *vs.* distance using gray lines, and the bold lines show the best fit to the observed data from the theory. Later, Hoshiba (1993) proposed a single station method to develop three curves, where he used average coda power at a fixed lapse time for the source energy. Variations of the methods have been used to make simultaneous measurement of attenuation and scattering coefficient in the world. Seismic albedo B_0 has been found to vary from 0.2 to 0.8 and Q_S^{-1} decreases with increasing frequency over the range of 1–20 Hz.

F. Other studies of seismogram envelopes

The whole seismogram reflects not only the source information but also the scattering characteristics of the earth medium. Sato (1984) proposed to synthesize three-component seismogram envelopes by summing up single scattered waves' energy, where frequency–dependent nonisotropic scattering-amplitudes are calculated based on the Born approximation. S-coda amplitudes are large on all three components, where SS-scattering contributes significantly for a wide range of lapse times, and pseudo P- and S-phases appear even in the null direction. Later, Yoshimoto *et al.* (1997a, b) developed an envelope synthesis including the reflection at the free surface.

The conventional waveform inversion for the source process was not successful when applied to high-frequency seismograms. The appropriate approaches would be to disregard the phase information and focus instead on seismogram envelopes. Zeng *et al.* (1993) mapped the high-frequency radiation from the fault plane using seismogram envelope analysis based on geometrical ray theory. Gusev and Pavlov (1991) and Kakehi and Irikura (1996) proposed to use seismogram envelopes of small aftershocks as an empirical Green function. By using a solution of the radiative transfer equation, Nakahara *et al.* (1998) proposed an inversion method to estimate the spatial distribution of high-frequency energy radiation from the fault plane. Analyzing records of the 1994 off-Sanriku earthquake, Japan, they reported that the spatial distribution of high-frequency radiation does not always coincide with the slip distribution determined from longer period waves.

The duration of observed S-wave packet at distances longer than 100 km is much longer than the source duration and the peak amplitude is delayed after the first arrival (Sato, 1989). It was initially proposed that this envelope broadening is a propagation effect due to diffraction and forward scattering caused by slowly varying velocity structure, which was modeled by employing a stochastic treatment of the parabolic wave-equation (Lee and Jokipii, 1975a, b). Applying the theoretical prediction for the Gaussian ACF to envelope data observed at Kanto, Japan, Sato (1989) and Scherbaum and Sato (1991) estimated $\varepsilon^2 / a \approx 10^{-(2.98\sim3.27)}$ km^{-1}. Analyzing the characteristics of seismogram envelopes from a larger region in Japan, Obara and Sato (1995) found that the random inhomogeneity in the back-arc side of the volcanic front is rich in short wavelength components compared with the Gaussian spectra. Gusev and Abubakirov (1997) reported a decrease of scattering coefficient with increasing depth revealed from the envelope broadening of both P- and S-waves in Kamchatka.

III. Spatial coherence of seismic array data

The common practice to deal with multi-scale, broadband heterogeneities in seismology is to smooth both the observed wave field and the heterogeneity model. In this way the information about small-scale heterogeneities is ignored and the obtained image can only recover the slowly varying, large-scale heterogeneities.

Stochastic methods, on the other hand, can obtain some statistical characteristics of the small-scale heterogeneities from the statistics of the wave field fluctuations. Statistical parameters of the medium include the RMS perturbation of velocity distribution, characteristic scale length, power spectrum or correlation function of velocity perturbations. Therefore, deterministic and stochastic methods are complimentary to each other when exploring multi-scale complex media. In the overlapping spectral band, the deterministic and stochastic methods are observing the same object from different aspects and using different simplifications during the analysis process.

The study of stochastic characteristics of random media using forward-scattered waves started a few decades ago. In the earlier studies (e.g. Nikolaev, 1975; Aki, 1973; Capon, 1974; Berteussen, 1975; Berteussen *et al*., 1975, 1977; MacLaughlin and Anderson, 1987), only variance and transverse coherence functions (TCF) of phase and amplitude fluctuations were used. Limited by the amount of information contained in these coherence functions, the medium model description is restricted to a single-layer of uniform, isotropic random medium. Through the use of the scattering theory of Chernov (1960), several statistical parameters, such as the RMS velocity perturbation, the average scale length and the total thickness of the layer, were inferred from the observed data. At the end of the 1980s, Flatté and Wu (1988) introduced a new statistical observable, the angular coherence function (AnCF), which increased significantly the statistical

information in the reduced data sets, and allowed the authors to derive a simple model of a layered, multi-scale random media. More recently, Wu (1989), Wu and Flatté (1990), and Chen and Aki (1991) introduced the new joint coherence function (JCF) or Joint transverse-angular coherence function (JTACF) and derived the theoretical relation between the joint coherence functions of array data and the heterogeneity spectrum (heterospectrum) of the random media. Wu and Xie (1991) conducted numerical experiments to test the performance of inverting JTACF to obtain the depth-dependent heterogeneity spectrum. The recent development in theory and methods increases greatly the amount of information in the utilized statistical data set and therefore improves significantly the model resolution, especially the depth resolution of the heterogeneity spectrum.

A. Observations of amplitude and phase fluctuations and their coherences

Due to wave diffraction, focusing and defocusing effects caused by heterogeneities in a medium, wave front distortion and fluctuations of various parameters of the wave field such as amplitude, arrival time and arrival angle may occur. Arrival time and amplitude fluctuations of waves crossing a seismic array such as NORSAR, LASA and other local or regional arrays have been widely observed. The pattern of fluctuations may change drastically even between nearly co-located events.

1. *Definitions of various coherence functions:* Coherence analysis is an effective method of describing statistical properties of the wave field. TCF defines the coherency (or similarity) of two transmitted wave fields as a function of horizontal separations between receivers; AnCF, defines the coherency as a function of angles between incident waves. For the more general case, the JTACF gives the measure of coherency between two transmitted wave fields with

different incident angles and observed at different stations (see Fig. 7). Compared with TCF and AnCF, JTACF changes the coherence data from a 1D to a 3D matrix (a function of station separation, dip, and azimuth angles) and therefore increases tremendously the information content of the coherence data set, providing more constraints for the determination of medium properties under the array. However, the advantage of increasing the resolving power is offset by decreasing the statistical stability to some degree. For real array data sets, the compromise between resolution and stability depends on the amount of data and angular coverage of the events. In practical array measurements the influence of array aperture to the calculation of coherence functions has to be taken into consideration (Flatté and Xie, 1992).

B. Theoretical basis of coherence analysis and inversion

The theory of transverse coherence of wave field after passing through a uniform random media has been available in the literature for a long time (Chernov, l960; Tatarskii, l971; Munk and Zacharasen, l976; Flatté *et. al*., l979). However, the formulations for angular coherence and for joint coherence functions has only been derived recently by Wu and Flatté (1990) using the Rytov approximation and Markov approximation. Chen and Aki (l99l) independently derived similar formulas using the Born approximation. The theory of the joint coherence functions includes the TCF and AnCF as special cases. In the derivations of Wu and Flatté (1990), spectral representation of random media is used and the depth dependency of the spectrum is introduced. Therefore, the new theory is more general and more suitable for the multi-scale, depth-dependent earth heterogeneities.

In transmission fluctuation analysis, only the initial P arrival (direct P, PKP or PKIKP) of a seismogram is used. By doing so, all the backscattered and large-angle scattered waves are neglected. Therefore, the problem becomes a

forward scattering or small-angle scattering problem, for which the scalar wave approximation can be used (Wu and Aki, 1985; Wu, 1989). In such scattering problems, only the wave speed perturbations affect the scattered field. Let the wave speed be $V(\mathbf{x}) = V_0\left[1+\xi(\mathbf{x})\right]$, where V_0 is the deterministic background velocity and $\xi(\mathbf{x})$ is the random perturbation. Let U_0 be the wavefield in the absence of fluctuations, and define the field perturbation Ψ by

$$U = U_0 e^{\Psi} \quad \text{and} \quad \Psi = \ln U - \ln U_0 = \ln\frac{A}{A_0} + i(\phi - \phi_0) = v + i\varphi \tag{9}$$

Substituting the above equation into the wave equation and taking the Rytov approximation and parabolic approximation, we derive the formulas for the *Joint Coherence Functions* (for the detailed derivation, see Wu and Flatté, 1990)

$$\begin{aligned}
\langle v_1 v_2\rangle\left(\mathbf{x}_T,\vec{\theta}\right) &= \frac{k^2}{4\pi^2}\int_0^H dz \iint_{-\infty}^{\infty} d\mathbf{k}_T e^{i\mathbf{k}_T\cdot(\mathbf{x}_T+z\vec{\theta})}\sin^2\frac{k_T^2 z}{2k}P(\mathbf{k}_T,0,z)\\
\langle \varphi_1 \varphi_2\rangle\left(\mathbf{x}_T,\vec{\theta}\right) &= \frac{k^2}{4\pi^2}\int_0^H dz \iint_{-\infty}^{\infty} d\mathbf{k}_T e^{i\mathbf{k}_T\cdot(\mathbf{x}_T+z\vec{\theta})}\cos^2\frac{k_T^2 z}{2k}P(\mathbf{k}_T,0,z)\\
\langle v_1 \varphi_2\rangle\left(\mathbf{x}_T,\vec{\theta}\right) &= \frac{k^2}{4\pi^2}\int_0^H dz \iint_{-\infty}^{\infty} d\mathbf{k}_T e^{i\mathbf{k}_T\cdot(\mathbf{x}_T+z\vec{\theta})}\sin\frac{k_T^2 z}{2k}\cos\frac{k_T^2 z}{2k}P(\mathbf{k}_T,0,z)
\end{aligned} \tag{10}$$

where $\mathbf{x}_T = \mathbf{x}_{T1} - \mathbf{x}_{T2}$ is the receiver separation vector (transverse separation), $\vec{\theta} = (\vec{\theta}_1 - \vec{\theta}_2)$ is the incident-angle separation vector, H is the propagation range in the random medium, here equal to the thickness of the random layer, $k_T = |\mathbf{k}_T|$ is transverse wavenumber and $P(\mathbf{k}_T, k_z, z)$ is the 3D power spectrum of the random heterogeneities $\xi(\mathbf{x})$ at depth z. Eq. (10) gives the general formulas for coherence analysis. Putting $\mathbf{x}_T = 0$ and $\vec{\theta} = 0$ in the above formulas, we obtain the variances and covariance of the fluctuations (magnitudes of fluctuations). For the transverse coherence of the fluctuations, we put $\vec{\theta} = 0$ into Eq. (10). For the angular coherence between fluctuations for two incident plane waves with angular separation of $\vec{\theta}$, we put $\mathbf{x}_T = 0$. In the past, the space domain formulation of Chernov (1960) was used for fluctuation analysis. Explicit expressions were derived for the case of a Gaussian ACF by Chernov (see also, Sato and Fehler,

l998). The corresponding formulas can be obtained by substituting a Gaussian PSDF into Eq. (10).

C. Inversion for statistical characteristics of earth heterogeneities

1. *Estimations of turbidity in the crust and upper* mantle: In the l960's, Russian scientists conducted extensive investigations using the log-amplitude fluctuation of P-wave first motion from explosions and earthquakes to infer the crustal and upper mantle "turbidity coefficients" at different depths (see Nikolaev, l975). The turbidity coefficient is defined as the variance of log-amplitude fluctuations produced by a unit travel distance. The depth of heterogeneities contributing to the measured turbidity was estimated by determining the seismic ray travel paths. In these measurements, the turbidity coefficients were rather phenomenological or apparent parameters which might have included spatial variations of site factors and the variations of intrinsic attenuation. Nikolaev (l975) concludes that the turbidity for 5 Hz P-waves in the crust and upper mantle is 0.0001–0.0025 km^{-1}, with an error factor of about two.

2. *Uniform random medium model for the lithosphere*: For the single layer Gaussian medium model, the model parameters are the RMS velocity perturbation ε, correlation length a and the layer thickness H. Correlation length a can be estimated from a measurement of the transverse correlation of log amplitude and phase. The layer thickness H and the wave speed perturbation ε can be obtained from the measured variance and covariance of v and φ. This single layer isotropic Gaussian medium model has been used to analyze the data at LASA (Aki, l973; Capon, l974; Berteussen *et al.,* 1975) NORSAR (Capon and Berteussen, l974; Berteussen *et al*., l977), and the Gauribindanur seismic array (GBA) in Southern India (Berteussen *et al*., l977). It is found that the estimate of correlation length a is much better constrained than the layer thickness H and

perturbation ε. For LASA, $a \approx$10-12 km, but H ranged from 60 km to 120 km with ε varying from 4% to 1.9% from different investigations.

3. *Non-Gaussian nature of the heterogeneities*: The Gaussian correlation function characterizes single-scale smoothly heterogeneous media, while real heterogeneities in the earth are often multi-scaled. Flatté and Wu (l988) showed that the exponential or Kolmogorov correlation functions fit the data much better than the Gaussian correlation function. The non-Gaussian nature of the lithospheric heterogeneities has been established also from velocity well-logging data (Sato, l979; Wu, l982).

4. *Depth dependent random medium model for the crust and upper mantle*: As many investigators pointed out (Berteussen *et al.,* l975; Flatté and Wu, l988; Wu and Flatté, l990), the use of only TCF resulted in poor determination of the random medium thickness and the ambiguity in resolving the medium perturbation strength (variances) and the thickness. After introducing the AnCF, Flatté and Wu (l988) were able to invert both the TCF and AnCF for a more complex random medium model. They showed that a single-layer uniform random medium failed to explain the observed fluctuation coherences represented by both TCF and AnCF and proposed a two-layer (overlapping) random medium model for the crust and upper mantle beneath the NORSAR (see Fig. 8). Each layer has a different perturbation strength and a different power-law heterogeneity spectrum. The best model has the top layer extending to a depth of 200 km with a flat spectrum, representing the small-scale heterogeneities in the lithosphere, and the second layer located between 15 and 250 km with a k^{-4} power-law spectrum, where k is wavenumber. The latter spectrum characterizes the large-scale heterogeneities in the mantle. From the RMS travel-time fluctuation (0.135 s) and the RMS log-amplitude fluctuation (0.41 neper= 3.6 dB), the RMS P -wave

speed perturbation for the first layer is 0.9–2.2% and for the second layer, 0.5–1.3%.

Based on the theory of general coherence analysis in random media, it is clear that TCF has no depth resolution and AnCF has only limited depth resolution that degenerates quickly with increasing depths. On the other hand, the joint coherency functions (JCF) increase tremendously the information content and provide high depth resolution. JTACF have been calculated for the NORSAR data (Wu *et al*., l994) and the Southern California Seismic Network data (Liu *et al*., l994; Wu *et al*., l995), and some interesting findings were reported.

IV. Numerical modeling of wave propagation in heterogeneous media

We have presented some analytical methods for investigating wave propagation in heterogeneous media where only the random component of heterogeneity is modeled. Generally, modeling random heterogeneities with deterministic structures using the methods discussed is difficult. In addition, for studies of wave propagation in random media, we usually model the mean response of a suite of random media whose statistical characterizations are the same. Results from such modeling are often difficult to relate to real earth observations. We now briefly discuss numerical modeling of wave propagation in heterogeneous media.

Numerous modeling studies have been undertaken to investigate wave propagation in heterogeneous media using numerical modeling. Numerical methods can model a wide range of earth structures. Studies using finite difference (Frankel and Clayton, 1986; Shapiro and Kneib, 1993), boundary integral approach (Benites *et al.*, 1992; Benites *et al.*, 1997), homogeneous layer solutions (Richards and Menke, 1983), and Fourier domain methods (Spivack and Uscinski, 1989; Hoshiba 1999; Wu *et al.*, 2000) have been made. In each case,

the choice of numerical method was based on the type of wave phenomena being investigated. Boundary integral and finite difference solutions provide reliable solutions including all wave field phenomena in strongly heterogeneous media; however, both methods are computationally expensive and it is difficult to investigate a range of models. For example, finite difference solutions require that grid spacing be chosen to minimize grid dispersion. As the propagation times and frequency being modeled increase, the spatial grid size and time increment must decrease to minimize grid dispersion (Holberg, 1987). As an example, Wu *et al.* (2000) required a grid spacing of 0.02 times the dominant wavelength to reliably model propagation to distances of 35 wavelengths. Boundary integral approaches have restrictions on the number of fictitious sources required along each boundary to adequately match boundary conditions. As velocity heterogeneity or frequency increase, the number of fictitious sources increases and the resulting computational cost increases.

Since several complete descriptions of finite difference and boundary integral techniques are available (Holberg, 1987; Benites *et al.*, 1992), we will discuss a class of numerical modeling techniques that has received little attention among seismologists. The methods are powerful in that they can model wave propagation faster than can be done using finite difference or boundary integral approaches. The methods have been extensively used in seismic exploration since the introduction of an intuitive approach for seismic wave modeling known as phase shift plus interpolation (PSPI) by Gazdag and Sguazzero (1984) and the work of Stoffa *et al.* (1990), who extended a wave-equation based method that was well known in acoustics (see e. g. Jensen *et al.*, 1994). The method of Stoffa *et al.* (1990) is called the Split-step Fourier (SSF) approach; its reliability has been quantitatively investigated by Huang and Fehler (1998). Extensions of the SSF method have been presented by Wu (1994), Huang *et al*. (1999a, 1999b), Huang and Fehler (1999) and Wu *et al.* (2000). The methods are reliable for

modeling wave propagation in the forward direction but the effects of reverberations between scatterers are not included. The methods operate in the frequency domain and calculations are performed in the wavenumber and space domains. We will briefly introduce the SSF approach.

A. SSF approach

The constant-density scalar-wave equation in the frequency domain is

$$\left[\frac{\partial^2}{\partial x^2}+\frac{\partial^2}{\partial y^2}+\frac{\partial^2}{\partial z^2}+\frac{\omega^2}{V(\mathbf{x}_T,z)^2}\right]U(\mathbf{x}_T,z;\omega)=0 \tag{11}$$

where $\mathbf{x}_T \equiv (x,y)$, $U(\mathbf{x}_T,z;\omega)$ is the wave field in the frequency domain, $V(\mathbf{x}_T,z)$ is the velocity of the medium, and ω is the angular frequency. In some sense we can break the scalar wave equation into two parts, one representing downgoing waves and one representing upgoing waves. The equation for downgoing waves is

$$\frac{\partial}{\partial z}U(\mathbf{x}_T,z;\omega)=i\,\Lambda(\mathbf{x}_T,z;\omega)\,U(\mathbf{x}_T,z;\omega) \tag{12}$$

where the positive z direction is the propagation direction and the square-root operator Λ is defined by

$$\Lambda(\mathbf{x}_T,z;\omega)=\sqrt{\frac{\omega^2}{V(\mathbf{x}_T,z)^2}+\frac{\partial^2}{\partial x^2}+\frac{\partial^2}{\partial y^2}} \tag{13}$$

The formal split-step marching solution of the one-way wave equation is given by

$$U(\mathbf{x}_T,z_i+\Delta z;\omega)=e^{\,i\int_{z_i}^{z_i+\Delta z}\Lambda(\mathbf{x}_T,z;\omega)dz}\,U(\mathbf{x}_T,z_i;\omega) \tag{14}$$

where we assume we know the wave field at z_i and we wish to compute the wave field at $z_i+\Delta z$. Huang and Fehler (1998) discuss how to use a small-angle approximation to evaluate the exponential of the integral in Eq. (14) to obtain

$$U(\mathbf{x}_T,z_{i+1};\omega)=e^{\,i\omega\left[\int_{z_i}^{z_{i+1}}\Delta s(\mathbf{x}_T,z)\,dz\right]}U_0(\mathbf{x}_T,z_{i+1};\omega) \tag{15}$$

where the slowness heterogeneity $\Delta s \equiv 1/V(\mathbf{x}_\perp,z)-1/V_0(z)$ is assumed to be small, and $U_0(\mathbf{x}_T,z_{i+1};\omega)$ is the wave field at z_{i+1} obtained by propagation of the

wave field across the interval Δz where the interval is assumed to have homogeneous velocity V_0 and

$$U_0(\mathbf{x}_T, z_{i+1}; \omega) = F_{\mathbf{k}_T}^{-1}\left\{e^{ik_z(z_i)\Delta z} F_{\mathbf{x}_T}\{U(\mathbf{x}_T, z_i, \omega\}\right\} \quad (16)$$

where $k_z(z_i) = \sqrt{k_0(z_i)^2 - \mathbf{k}_T^2}$ and $k_0 = \omega / V_0(z_i)$. $F_{\mathbf{x}_T}$ and $F_{\mathbf{k}_T}^{-1}$ are 2D Fourier and inverse Fourier transforms over $\mathbf{x}_T$ and $\mathbf{k}_T$, respectively. Wave propagation is done in two steps: a free space propagation in the wavenumber domain across each depth interval using the background slowness s_0 for the interval followed by a correction for the heterogeneity described by Δs within the propagation interval, which is done in the space domain. The wave field is transferred between the space and wavenumber domains using a Fast Fourier Transform. Since the propagator depends only on the local medium properties, access to the entire velocity structure of a model is not required to propagate through a portion of the model. This gives the method a computational advantage over some other wave-equation-based methods. The method is valid for extrapolating the wave field so long as the primary direction of propagation is nearly parallel to the positive z direction and the variation in velocity is small in the direction perpendicular to z. Later extensions mentioned above have systematically improved the accuracy for large-angle waves in strongly varying media.

The SSF method has been used by Hoshiba (1999) in an investigation of the influences of random structure on amplitudes of seismic waves. Wu *et al.* (2000) developed a method similar to the SSF method for modeling Lg propagation in heterogeneous media. Spivack and Uscinski (1989) present an analytic and numerical investigation of the accuracy of the SSF method and conclude that it is reliable for calculating wave fields in random media but that it is even more reliable when computing transverse correlations of the wave field. There is a stochastic treatment of the phase screen method, which is called the Markov approximation (Sreenivasiah *et al.*, 1976; Lee and Jokipii, 1975a, b). This method directly gives the wave envelope in random media, and is applied to

the study of seismogram-envelope characteristics (Sato, 1989, Scherbaum and Sato, 1991; Obara and Sato, 1995). Fehler *et al.* (2000) have compared waveforms calculated for random media using finite difference, an extension of the SSF method, and the Markov approximation.

V. Summary and Discussion

Beginning from visual observations of the character of recorded seismograms that led to new ways of thinking about seismic wave propagation, the study of seismic wave scattering and attenuation has led to new and improved observational tools for characterizing the earth. One reason that the coda normalization method has been so useful is because station calibration and/or site amplification could be eliminated so that other medium parameters could be measured. Recent theories about seismic wave propagation in heterogeneous media can also be applied to investigate envelope shape and additional information about lithospheric structure can be obtained from broadband calibrated data.

Table 1 summarizes fundamental observations that have led to advances in our understanding of stochastic wave phenomena in the earth's lithosphere. The model or interpretation method used to understand each fundamental observation is listed along with the parameters that can be estimated by application of the models to real data. Many of the parameters can be estimated using deterministic models. In most cases, observations made using deterministic and random-wave approaches are complementary. In many cases, the stochastic approach provides parameters characterizing the earth's lithosphere that cannot be obtained from deterministic measurements.

Our understanding about the structure of heterogeneity of the earth's lithosphere as a function of scale is limited. While some data can be explained using well-defined correlation functions that have a narrow-band of

heterogeneity, this does not mean that heterogeneity is limited to a narrow band. One fundamental issue facing those who investigate scattered waves is to find a unifying theory for a broad spectrum of seismic data that allows us to estimate the scale of heterogeneity over a broad range of scales.

Use of stochastic seismology has led to significant advances in our understanding of the character of seismic waveforms and enabled us to model portions of the waveforms that cannot be explained deterministically. The success of the models has improved our understanding of wave propagation in the earth and led to the prediction of parameters that improve our understanding the structure and composition of the Earth's lithosphere.

Key references (Full references are put in CD-ROM)

Aki, K. (1969). Analysis of seismic coda of local earthquakes as scattered waves, *J. Geophys. Res.* **74**, 615–631.

Aki, K. (1980). Attenuation of shear-waves in the lithosphere for frequencies from 0.05 to 25 Hz, *Phys. Earth Planet. Inter.* **21**, 50–60.

Aki, K. (l973). Scattering of P waves under the Montana Lasa, *J. Geophys. Res.* **78**, 1334-1246.

Aki, K. and Richards, P. (1980). "Quantitative Seismology - Theory and Methods", Vols. 1 and 2, W. H. Freeman, San Francisco.

Aki, K., and Chouet, B. (1975). Origin of coda waves: Source, attenuation and scattering effects, *J. Geophys. Res.* **80**, 3322–3342.

Anderson, D. L., and Hart, R. S. (1978). Q of the Earth, *J. Geophys. Res.* **83**, 5869–5882.

Benites, R. A., Roberts, P. M., Yomogida K., and Fehler, M. (1997). Scattering of elastic waves in 2-D composite media I. Theory and test, *Phys. Earth Planet Inter.*, **104,** 161-173.

Berteussen, K. A., Christoffersson, A., Husebye, E. S., and Dahle, A. (1975). Wave scattering theory in analysis of P wave anomalies at NORSAR and LASA, *Geophys. J. R. Astr. Soc*. **42**, 402-417.

Chernov, L. A. (1960). "Wave Propagation in a Random Medium" (Engl. trans. by R. A. Silverman). McGraw–Hill, New York.

Fehler, M., Roberts, P., and Fairbanks, T. (1988). A temporal change in coda wave attenuation observed during an eruption of Mount St. Helens, *J. Geophys. Res.* **93**, 4367–4373.

Fehler, M., Hoshiba, M., Sato, H., and Obara, K. (1992). Separation of scattering and intrinsic attenuation for the Kanto-Tokai region, Japan, using measurements of S-wave energy versus hypocentral distance, *Geophys. J. Int.* **108**, 787–800.

Fehler, M., Sato, H., and Huang, L.-J. (2000). Envelope broadening of outgoing waves in 2D random media: a comparison between the Markov approximation and numerical simulations, submitted.

Flatté, S. M., and Wu, R.-S. (1988). Small-scale structure in the lithosphere and asthenosphere deduced from arrival-time and amplitude fluctuations at NORSAR, *J. Geophys. Res.* **93**, 6601-6614.

Frankel, A., and Clayton, R. W. (1986). Finite difference simulations of seismic scattering: Implications for the propagation of short-period seismic waves in the crust and models of crustal heterogeneity, *J. Geophys. Res.* **91**, 6465–6489.

Frankel, A., and Wennerberg, L. (1987). Energy-flux model of seismic coda: Separation of scattering and intrinsic attenuation, *Bull. Seismol. Soc. Am*. **77**, 1223–1251.

Gazdag, J., and Sguazzero, P. (1984). Migration of seismic data by phase-shift plus interpolation, *Geophysics* , **49**, 124-131.

Gusev, A. A. (1995). Baylike and continuous variations of the relative level of the late coda during 24 years of observation on Kamchatka, *J. Geophys. Res*. **100**, 20311–20319.

Gusev, A. A., and Abubakirov, I. R. (1996). Simulated envelopes of non-isotropically scattered body waves as compared to observed ones: another manifestation of fractal heterogeneity, *Geophys. J. Int*., **127,** 49-60.

Hoshiba, M. (1991). Simulation of multiple-scattered coda wave excitation based on the energy conservation law, *Phys. Earth Planet. Inter.* **67**, 123–136.

Hoshiba M. (1993). Separation of scattering attenuation and intrinsic absorption in Japan using the multiple lapse time window analysis of full seismogram envelope, *J. Geophys. Res.* **98**, 15809–15824.

Huang, L.-J., and Fehler, M. (1998). Accuracy analysis of the split-step Fourier propagator: implications for seismic modeling and migration, *Bull. Seismol. Soc. Am.*, **88**, 8-28.

Huang, L.-J., Fehler, M., and Wu, R.-S. (1999a). Extended local Born Fourier migration, *Geophysics*, **64,** 1524-1534.

Huang, L.-J., Fehler, M., Roberts, P., and Burch, C. C. (1999b). Extended local Rytov Fourier migration method, *Geophysics*, **64,** 1535-1545.

Jackson, D. D., and Anderson, D. L. (1970). Physical mechanisms of seismic-wave attenuation, *Rev. Geophys. Space Phys.* **8**, 1–63.

Jin, A., and Aki, K. (1986). Temporal change in coda Q before the Tangshan earthquake of 1976 and the Haicheng earthquake of 1975, *J. Geophys. Res.* **91**, 665–673.

Jin, A., and Aki, K. (1989). Spatial and temporal correlation between coda Q^{-1} and seismicity and its physical mechanism, *J. Geophys. Res.* **94**, 14041–14059.

Kakehi, Y. and Irikura, K. (1996). Estimation of high-frequency wave radiation areas on the fault plane by the envelope inversion of acceleration seismograms, *Geophys. J. Int.* **125**, 892–900.

Kinoshita, S., (1994). Frequency-dependent attenuation of shear waves in the crust of the southern Kanto, Japan, *Bull. Seismol. Soc. Am.,* **84**, 1387-1396.

Kopnichev, Y. F. (1975). A model of generation of the tail of the seismogram, *Dok. Akad. Nauk, SSSR* (Engl. trans.) **222**, 333–335.

Liu, H., P., Anderson, D. L., and Kanamori, H. (1976). Velocity dispersion due to anelasticity; implications for seismology and mantle composition, *Geophys. J. R. Astron. Soc*. **47**, 41-58.

Mavko, G. M., and Nur, A. (1979). Wave attenuation in partially saturated rocks, *Geophysics*, **44**, 161–178.

Nakahara, H., Nishimura, T., Sato, H., and Ohtake, M. (1998). Seismogram envelope inversion for the spatial distribution of high-frequency energy radiation on the earthquake fault: Application to the 1994 far east off Sanriku earthquake (Mw=7.7). *J. Geophys. Res.* **103,** 855-867.

Nikolaev, A. V. (1975). "The Seismics of Heterogeneous and Turbid Media " (Engl. trans. by R. Hardin), Israel Program for Science translations, Jerusalem.

Nishigami, K. (1991). A new inversion method of coda waveforms to determine spatial distribution of coda scatterers in the crust and uppermost mantle, *Geophys. Res. Lett*. **18**, 2225–2228.

Obara, K., and Sato, H. (1995). Regional differences of random inhomogeneities around the volcanic front in the Kanto-Tokai area, Japan, revealed from the broadening of S wave seismogram envelopes, *J. Geophys. Res.* **100**, 2103–2121.

O'Connell, R. J., and Budiansky, B. (1977). Viscoelastic properties of fluid-saturated cracked solids, *J. Geophys. Res.* **82**, 5719–5735.

Phillips, W. S., and Aki, K. (1986). Site amplification of coda waves from local earthquakes in central California, *Bull. Seismol. Soc. Am*. **76**, 627–648.

Rautian, T. G., and Khalturin, V. I. (1978). The use of the coda for determination of the earthquake source spectrum, *Bull. Seismol. Soc. Am.* **68**, 923–948.

Roth, M., and Korn, M. (1993). Single scattering theory versus numerical modelling in 2-D random media, *Geophys. J. Int.* **112**, 124–140.

Sato, H. (1977). Energy propagation including scattering effect: Single isotropic scattering approximation, *J. Phys. Earth* **25**, 27–41.

Sato, H. (1982). Amplitude attenuation of impulsive waves in random media based on travel time corrected mean wave formalism, *J. Acoust. Soc. Am.* **71**, 559–564.

Sato, H. (1984). Attenuation and envelope formation of three-component seismograms of small local earthquakes in randomly inhomogeneous lithosphere, *J. Geophys. Res.* **89**, 1221–1241.

Sato, H. (1989). Broadening of seismogram envelopes in the randomly inhomogeneous lithosphere based on the parabolic approximation: Southeastern Honshu, Japan, *J. Geophys. Res.* **94**, 17735–7747.

Sato, H., and Fehler, M. (1998). "*Seismic Wave Propagation and Scattering in the Heterogeneous Earth*", AIP Preess/ Springer Verlag, New York.

Sato, H., Nakahara, H., and Ohtake, M. (1997). Synthesis of scattered energy density for non-spherical radiation from a point shear dislocation source based on the radiative transfer theory, *Phys. Earth Planet. Inter*. **104,** 1-14.

Scherbaum, F., and Sato, H. (1991). Inversion of full seismogram envelopes based on the parabolic approximation: Estimation of randomness and attenuation in southeast Honshu, Japan, *J. Geophys. Res.* **96**, 2223–2232.

Shapiro, S. A., and Kneib, G. (1993). Seismic attenuation by scattering: Theory and numerical results, *Geophys. J. Int.* **114**, 373–391.

Stoffa, P., Fokkema, J., de Luna Friere, R., and Kessinger, W. (1990). Split-step Fourier migration, *Geophysics*, **55**, 410-421.

Tsujiura, M. (1978). Spectral analysis of the coda waves from local earthquakes, *Bull. Earthq. Inst. Univ. Tokyo* **53**, 1–48.

Wu, R.-S. (1982). Attenuation of short period seismic waves due to scattering, *Geophys. Res. Lett.* **9**, 9–12.

Wu, R.-S. (1985). Multiple scattering and energy transfer of seismic waves - separation of scattering effect from intrinsic attenuation - I. Theoretical modeling, *Geophys. J. R. Astron. Soc.* **82**, 57–80.

Wu, R.-S. (1989). The perturbation method for elastic waves scattering, *Pure Applied Geophys*. **131**, 605-637.

Wu, R. S. (1994).Wide-angle elastic wave one-way propagation in heterogeneous media and elastic wave complex-screen method, *J. Geophys. Res.,* **99**, 751-766.

Wu, R.-S., and Flatté, S. M. (1990). Transmission fluctuations across an array and heterogeneities in the crust and upper mantle, *Pure Applied Geophys*. **132**, 175-196.

Wu, R.-S., and Xie, X. B. (1991). Numerical tests of stochastic tomography, *Phys. Earth & Planet. Int*., **67**, 180-193.

Wu, R.-S., Jin, S., and Xie, X.-B. (2000). Seismic wave propagation and scattering in heterogeneous crustal waveguides using screen propagators: I SH waves, *Bull. Seismol. Soc. Am.*, in press.

Yoshimoto, K., Sato, H., and Ohtake, M. (1993). Frequency-dependent attenuation of P and S waves in the Kanto area, Japan, based on the coda-normalization method, *Geophys. J. Int.* **114**, 165–174.

Yoshimoto, K., Sato, H., and Ohtake, M. (1997b). Short-wavelength crustal inhomogeneities in the Nikko area, central Japan, revealed from the three-component seismogram envelope analysis, *Phys. Earth Planet. Inter.* **104,** 63-74.

Zener, C. (1948). “Elasticity and Anelasticity of Metals”, University of Chicago Press, Chicago.

Zeng, Y., Su, F., and Aki, K. (1991). Scattering wave energy propagation in a random isotropic scattering medium 1. Theory, *J. Geophys. Res.* **96**, 607–619.

Zeng, Y., Aki, K. and Teng, T. L. (1993). Mapping of the high-frequency source radiation for the Loma Prieta earthquake, California, *J. Geophys. Res.* **98,** 11981–11993.

Table 1. Fundamental observations that have led to advances in using stochastic seismology to model scattered waves, theory and methods used to explain the observations, and the parameters that may be inferred from the methods.

Observation	**Theory and Interpretation Method**	**Parameters Estimated**
Existence of Coda	• Phenomenological • Coda Normalization Method • Single scattering Approximation • Energy-Flux Model	• Coda Attenuation • Scattering Coefficient • Relative Site Amplification • Relative Source Factors
Envelope Shape of Local Earthquakes	• Radiative Transfer Theory • Multiple Lapse-Time Window Analysis	• Scattering Coefficient • Seismic Albedo (Scattering Loss, Intrinsic Absorption) • High Frequency Radiation from Fault
Attenuation	• Spectral Decay with Distance • Coda Normalization Method • Born Approximation	• Fractional Velocity Fluctuation • Scale Length (Correlation length) of Heterogeneity • Spectra of Heterogeneity • Spatial Variation of Stochastic Characterization of Medium
Array Phase/ Amplitude Characteristics	• Diffraction/Forward Scattering • Parabolic Wave Equation and Rytov-Approximation • Theory of Coherence Analysis	
Envelope Broadening of Regional Seismograms	• Diffraction/Forward Scattering • Parabolic Wave Equation • Markov Approximation	

FIGURE 1 a. Reported values of Q_S^{-1} for the lithosphere: surface wave analysis, 1-7; multiple lapse-time window analysis, 8-12; spectral decay analysis, 11-26. **b.** Reported values of Q_P^{-1} for the lithosphere: surface-wave analysis, 1; spectral decay analysis, 2-8; extended coda-normalization method, 9-10. Detailed references are given by Sato and Fehler (1998). [Reprinted from Sato and Fehler (1998) with permission from Springer-Verlag].

FIGURE 2. Scattering attenuation *vs.* ak for scalar waves: dotted curve, the ordinary Born approximation; solid curves, the corrected Born approximation, where $k = \omega / V_0$. $\psi_C = 90^\circ$ by Wu [1982a] and $\psi_C \approx 29^\circ$ by Sato [1982].

FIGURE 3. Horizontal-component velocity seismograms of a crustal earthquake of M_L=4.6 in Japan. Seismograms are arranged from bottom to top by increasing distance from the earthquake epicenter. The direct S-wave is followed by S-coda waves [Courtesy of K. Obara].

FIGURE 4 a. Geometry of the multiple scattering process for a point-shear dislocation source, where the lobes show the radiation pattern of the S-wave energy. **b.** Temporal change in the normalized energy density at $r = 1/g_0$ at different directions from a point shear-dislocation source, where $\bar{t} = g_0 V_0 t$. The broken curve corresponds to results for spherical source radiation [Reprinted from Sato *et al.* (1997) with permission from Elsevier Science].

FIGURE 5. a. Coda attenuation Q_C^{-1} against frequency for various regions. **b.** Total scattering coefficient g_0 for SS scattering *vs.* frequency from regional measurements made throughout the world: results obtained using the single scattering model are labeled 1-5 (plots include backscattering coefficient g_π); results based on the multiple lapse-time window analysis (Isotropic scattering is assumed) are labeled 6-8. Detailed references are given by Sato and Fehler (1998) [Reprinted from Sato and Fehler (1998) with permission from Springer-Verlag].

FIGURE 6. Normalized integrated energy density with geometrical spreading correction *vs.* hypocentral distance in the Kanto–Tokai region, Japan, relative to the value at a hard rock borehole site for vertical component data. Average of data and best fit theoretical curves are

shown by gray lines and bold curves, respectively for 4–8 Hz band [Reprinted from Fehler *et al.* (1992) with permission from Blackwell Science].

FIGURE 7. Comparison of the data reduction geometry for TCF (transverse coherence function), AnCF (angular coherence function), and JTACF (joint transverse-angular coherence function).

FIGURE 8. Comparison between the data and the prediction of the two-layered power-law random medium model at NORSAR: **a.** TCF; **b**. AnCF [Reprinted from Flatté and Wu (1988) with permission from American Geophysical Union].

Full References for CD-ROM (Papers marked by * are printed.)

*Aki, K. (1969). Analysis of seismic coda of local earthquakes as scattered waves, *J. Geophys. Res.* **74**, 615–631.

*Aki, K. (l973). Scattering of P waves under the Montana Lasa, *J. Geophys. Res.* **78**, 1334-1246.

*Aki, K. (1980). Attenuation of shear-waves in the lithosphere for frequencies from 0.05 to 25 Hz, *Phys. Earth Planet. Inter.* **21**, 50–60.

*Aki, K., and Chouet, B. (1975). Origin of coda waves: Source, attenuation and scattering effects, *J. Geophys. Res.* **80**, 3322–3342.

*Aki, K. and Richards, P. (1980). "Quantitative Seismology - Theory and Methods", Vols. 1 and 2, W. H. Freeman, San Francisco.

Al-Shukri, H. J. and Mitchell, B. J. (1990). Three dimensional attenuation structure in and around the New Madrid seismic zone, *Bull. Seismol. Soc. Amer.*, **80**, 615-632.

*Anderson, D. L., and Hart, R. S. (1978). Q of the Earth, *J. Geophys. Res.* **83**, 5869–5882.

Aster, R, C., Slad, G., Henton, J., and Antolik, M. (1996). Differential analysis of coda Q using similar microearthquakes in seismic gaps. Part 1: Techniques and application to seismograms recorded in the Anza Seismic Gap, *Bull. Seismol. Soc. Am.* **86**, 868–889.

*Benites, R., Aki K., and Yomogida, K., (1992). Multiple scattering of SH waves in 2-D media with many cavities, *Pure Appl. Geophys.* **138**, 353–390.

Benites, R. A., Roberts, P. M., Yomogida K., and Fehler, M. (1997). Scattering of elastic waves in 2-D composite media I. Theory and test, *Phys. Earth Planet Inter.*, **104,** 161-173.

Berteussen, K. A. (1975). Crustal structure and P-wave travel time anomalies at NORSAR, *J. Geophys*. **41**, 71-84.

*Berteussen, K. A., Christoffersson, A., Husebye, E. S., and Dahle, A. (1975). Wave scattering theory in analysis of P wave anomalies at NORSAR and LASA, *Geophys. J. R. Astr. Soc*. **42**, 402-417.

Berteussen, K. A., Husebye, E. S., Mereu, R. F., and Ram, A. (1977). Quantitative assessment of the crust-upper mantle heterogeneities beneath the Gauribidanur seismic array in Southern India, *Earth and Planet. Sci. Lett*. **37**, 326-332.

Biswas, N. N., and Aki, K., (1984). Characteristics of coda waves: Central and south central Alaska, *Bull. Seismol. Soc. Am.* **74**, 493–507.

Capon, J. (1974). Characterization of crust and upper mantle structure under LASA as a random medium, *Bull. Seismol. Soc. Am*. **64**, 235-266.

Capon, J., and Berteussen, K. A. (1974). A random medium analysis of crust and upper mantle structure under NORSAR, *Geophys. Res. Lett.* **1**, 327-328.

Carpenter, P. J. and Sanford, A. R. (1985). Apparent Q for upper crustal rocks of the Central Rio Grande Rift, *J. Geophys. Res.* **90**, 8661–8674.

Chen, X. and Aki, K. (1991). General coherence functions for amplitude and phase fluctuations in a randomly heterogeneous medium, *Geophys. J. Int.* **105**, 155–162.

*Chernov, L. A. (1960). "Wave Propagation in a Random Medium" (Engl. trans. by R. A. Silverman). McGraw–Hill, New York.

Chouet, B. (1979). Temporal variation in the attenuation of earthquake coda near Stone Canyon, California, *Geophys. Res. Lett.* **6**, 143–146.

Clawson, S. R., Smith, R. B., and Benz, H. M. (1989). P wave attenuation of the Yellowstone Caldera from three-dimensional inversion of spectral decay using explosion source seismic data, J. Geophys. Res., **94**, 7205-7222.

Dewberry, S. R., and Crosson, R. S. (1995). Source scaling and moment estimation for the Pacific Northwest seismograph network using S-coda amplitudes, *Bull. Seismol. Soc. Am.* **85**, 1309–1326.

Dziewonski, A. M. (1979). Elastic and anelastic structure of the earth, *Rev. Geophys. Space Phys.* **17**, 303–312.

Ellsworth, W. L. (1991). Review for “Temporal change in scattering and attenuation associated with the earthquake occurrence - A review of recent studies on coda waves (H. Sato)”, in “Evaluation of Proposed Earthquake Precursors” (M. Wyss, Ed.). pp. 54–55, AGU, Washington, D. C.

Fang, Y., and Müller, G. (1996). Attenuation operators and complex wave velocities for scattering in random media, *Pure Appl. Geophys.* **148**, 269–285.

*Fehler, M., Roberts, P., and Fairbanks, T. (1988). A temporal change in coda wave attenuation observed during an eruption of Mount St. Helens, *J. Geophys. Res.* **93**, 4367–4373.

*Fehler, M., Hoshiba, M., Sato, H., and Obara, K. (1992). Separation of scattering and intrinsic attenuation for the Kanto-Tokai region, Japan, using measurements of S-wave energy versus hypocentral distance, *Geophys. J. Int.* **108**, 787–800.

*Fehler, M., Sato, H., and Huang, L.-J. (2000). Envelope broadening of outgoing waves in 2D random media: a comparison between the Markov approximation and numerical simulations, submitted.

Flatté, S. M., and Xie, X.-B. (1992). The transverse coherence function at NORSAR over a wide range of separations, *Geophys. Res. Lett.* **19**, 557-560.

Flatté, S. M., Dashen, R., Munk, W. H., Watson, K. M., and Zachariasen, F., (1979). *“Sound Transmission Through a Fluctuating Ocean”*, Cambridge, University Press, New York.

*Flatté, S. M., and Wu, R.-S. (1988). Small-scale structure in the lithosphere and asthenosphere deduced from arrival-time and amplitude fluctuations at NORSAR, *J. Geophys. Res.* **93**, 6601-6614.

Frankel, A. (1991). Review for "Observational and physical basis for coda precursor (Jin, A. and K. Aki)" in "Evaluation of Proposed Earthquake Precursors" (M. Wyss, Ed.), pp. 51–53, AGU, Washington, D. C.

*Frankel, A., and Clayton, R. W. (1986). Finite difference simulations of seismic scattering: Implications for the propagation of short-period seismic waves in the crust and models of crustal heterogeneity, *J. Geophys. Res.* **91**, 6465–6489.

*Frankel, A., and Wennerberg, L. (1987). Energy-flux model of seismic coda: Separation of scattering and intrinsic attenuation, *Bull. Seismol. Soc. Am*. **77**, 1223–1251.

*Gazdag, J., and Sguazzero, P. (1984). Migration of seismic data by phase-shift plus interpolation, *Geophysics* , **49**, 124-131.

Got, J. L., Poupinet, G., and Fréchet, J. (1990). Changes in source and site effects compared to coda Q^{-1} temporal variations using microearthquakes doublets in California, *Pure Appl. Geophys.* **134**, 195–228.

*Gusev, A. A. (1995). Baylike and continuous variations of the relative level of the late coda during 24 years of observation on Kamchatka, *J. Geophys. Res*. **100**, 20311–20319.

Gusev, A. A., and Pavlov, V. M. (1991). Deconvolution of squared velocity waveform as applied to study of non-coherent short-period radiator in earthquake source, *Pure Appl. Geophys*. **136**, 236–244.

*Gusev, A. A., and Abubakirov, I. R. (1996). Simulated envelopes of non-isotropically scattered body waves as compared to observed ones: another manifestation of fractal heterogeneity, *Geophys. J. Int*., **127,** 49-60.

Gusev, A. A., and Abubakirov, I. R. (1997). Study of the vertical scattering properties of the lithosphere based on the inversion of P- and S-wave pulse broadening data, *Volc. Seis.,* **18,** 453-464.

Hartse, H., Phillips, W. S., Fehler, M. C., and House, L. S. (1995). Single-station spectral discrimination using coda waves, *Bull. Seismol. Soc. Am.* **85**, 1464–1474.

Holberg, O. (1987). Computational aspects of the choice of operator and sampling interval for numerical differentiation in large-scale simulation of wave phenomena, *Geophysical Prospecting*, **35**, 629-655.

*Hoshiba, M. (1991). Simulation of multiple-scattered coda wave excitation based on the energy conservation law, *Phys. Earth Planet. Inter.* **67**, 123–136.

*Hoshiba M. (1993). Separation of scattering attenuation and intrinsic absorption in Japan using the multiple lapse time window analysis of full seismogram envelope, *J. Geophys. Res.* **98**, 15809–15824.

Hoshiba, M. (1999). Large fluctuation of wave amplitude produced by small fluctuation of velocity structure, preprint.

*Huang, L.-J., and Fehler, M. (1998). Accuracy analysis of the split-step Fourier propagator: implications for seismic modeling and migration, *Bull. Seismol. Soc. Am.*, **88**, 8-28.

*Huang, L.-J., Fehler, M., and Wu, R.-S. (1999a). Extended local Born Fourier migration, *Geophysics*, **64,** 1524-1534.

*Huang, L.-J., Fehler, M., Roberts, P., and Burch, C. C. (1999b). Extended local Rytov Fourier migration method, *Geophysics*, **64,** 1535-1545.

Huang, L.-J. and Fehler, M. (1999). Quasi-Born Fourier migration, in press in *Geophys. J. Int.*

*Jackson, D. D., and Anderson, D. L. (1970). Physical mechanisms of seismic-wave attenuation, *Rev. Geophys. Space Phys.* **8**, 1–63.

Jensen, F., Kuperman, A., Porter, M., and Schmidt, H. (1994). "Computational Ocean Acoustics", AIP Press, New York.

*Jin, A., and Aki, K. (1986). Temporal change in coda Q before the Tangshan earthquake of 1976 and the Haicheng earthquake of 1975, *J. Geophys. Res.* **91**, 665–673.

Jin, A., and Aki, K. (1988). Spatial and temporal correlation between coda Q and seismicity in China, *Bull. Seismol. Soc. Am.* **78**, 741–769.

*Jin, A., and Aki, K. (1989). Spatial and temporal correlation between coda Q^{-1} and seismicity and its physical mechanism, *J. Geophys. Res.* **94**, 14041–14059.

*Kakehi, Y. and Irikura, K. (1996). Estimation of high-frequency wave radiation areas on the fault plane by the envelope inversion of acceleration seismograms, *Geophys. J. Int.* **125**, 892–900.

Kawahara, J., and Yamashita, T. (1992). Scattering of elastic waves by a fracture zone containing randomly distributed cracks, *Pure Appl. Geophys*. **139**, 121–144.

Kikuchi, M. (1981). Dispersion and attenuation of elastic waves due to multiple scattering from cracks, *Phys. Earth Planet. Inter.* **27**, 100–105.

*Kinoshita, S., (1994). Frequency-dependent attenuation of shear waves in the crust of the southern Kanto, Japan, *Bull. Seismol. Soc. Am.*, **84**, 1387-1396.

Knopoff, L. (1964). Q, *Rev. Geophys*. **2**, 625–660.

*Kopnichev, Y. F. (1975). A model of generation of the tail of the seismogram, *Dok. Akad. Nauk, SSSR* (Engl. trans.) **222**, 333–335.

Leary, P., and Abercrombie, R. (1994). Frequency dependent crustal scattering and absorption at 5–160 Hz from coda decay observed at 2.5 km depth, *Geophys. Res. Lett*. **21**, 971–974.

Lee, L. C., and Jokipii, J. R. (1975a). Strong scintillations in astrophysics. I. The Markov approximation, its validity and application to angular broadening, *Astrophys. J.* **196**, 695–707.

Lee, L. C. and Jokipii, J. R. (1975b). Strong scintillations in astrophysics. II. A theory of temporal broadening of pulses, *Astrophys. J.* **201**, 532–543.

*Liu, H., P., Anderson, D. L., and Kanamori, H. (1976). Velocity dispersion due to anelasticity; implications for seismology and mantle composition, *Geophys. J. R. Astron. Soc*. **47**, 41-58.

Liu, X. P., Wu, R.-S., and Xie, X. B. (1994). Joint coherence function analysis of seismic travel times and amplitude fluctuations observed on southern California seismographic network and its geophysical significance, *EOS, Trans. Amer. Geophys. Union*, **75**, No. 44, 482.

Lundquist, G. M., and Cormier, V. C. (1980). Constraints on the absorption band model of *Q*, *J. Geophys. Res*. **85**, 5244–5256.

Matsumoto, S., and Hasegawa (1989). Two-dimensional coda Q structure beneath Tohoku, NE Japan, *Geophys. J. Int.* **99**, 101–108.

Matsunami, K. (1990). Laboratory measurements of spatial fluctuation and attenuation of elastic waves by scattering due to random heterogeneities, *Pure Appl. Geophys.* **132**,197–220.

*Mavko, G. M., and Nur, A. (1979). Wave attenuation in partially saturated rocks, *Geophysics*, **44**, 161–178.

McLaughlin, K. L. and Anderson, L. M. (1987). Stochastic dispersion of short-period P-waves due to scattering and multipathing, *Geophys. J. R. Astron. Soc*. **89**, 933–963.

Mitchell, B. J., Xie, Y.-P. J., andCong, L. (1997). Lg coda Q variation across Eurasia and its relation to crustal evolution, *J. Geophys. Res.*, **102**, 22767-22779.

Munk, W. H. and Zachariasen, F. (1976). Sound propagation through a fluctuating ocean-theory and observation, *J. Acous. Soc. Am*. **59**, 818-838.

*Nakahara, H., Nishimura, T., Sato, H., and Ohtake, M. (1998). Seismogram envelope inversion for the spatial distribution of high-frequency energy radiation on the earthquake fault: Application to the 1994 far east off Sanriku earthquake (Mw=7.7). *J. Geophys. Res.* **103,** 855-867.

*Nikolaev, A. V. (1975). "The Seismics of Heterogeneous and Turbid Media " (Engl. trans. by R. Hardin), Israel Program for Science translations, Jerusalem.

*Nishigami, K. (1991). A new inversion method of coda waveforms to determine spatial distribution of coda scatterers in the crust and uppermost mantle, *Geophys. Res. Lett*. **18**, 2225–2228.

Nur, A. (1971). Viscous phase in rocks and the low-velocity zone, *J. Geophys. Res.*, **76**, 1270-1277.

*Obara, K., and Sato, H. (1995). Regional differences of random inhomogeneities around the volcanic front in the Kanto-Tokai area, Japan, revealed from the broadening of S wave seismogram envelopes, *J. Geophys. Res.* **100**, 2103–2121.

*O'Connell, R. J., and Budiansky, B. (1977). Viscoelastic properties of fluid-saturated cracked solids, *J. Geophys. Res.* **82**, 5719–5735.

O'Doherty, K. B., Bean, C. J., and J Closkey, M. (1997). Coda wave imaging of the Log Valley caldera using a spatial stacking technique, *Geophys. Res. Lett.,* **24,** 1547-1550.

*Phillips, W. S., and Aki, K. (1986). Site amplification of coda waves from local earthquakes in central California, *Bull. Seismol. Soc. Am*. **76**, 627–648.

Ponko, S. C. and Sanders, C. O. (1994) Inversion for P and S wave attenuation structure, Long Valley caldera, California, *J. Geophys. Res.*, **99**, 2619-2635.

*Rautian, T. G., and Khalturin, V. I. (1978). The use of the coda for determination of the earthquake source spectrum, *Bull. Seismol. Soc. Am.* **68**, 923–948.

Revenaugh, J. (1995). The contribution of topographic scattering to teleseismic coda in Southern California, *Geophys. Res. Lett.,* **22**, 543-546.

Richards, P. G. and Menke, W. (1983). The apparent attenuation of a scattering medium, *Bull. Seismol. Soc. Am.* **73**, 1005–1021.

*Roth, M., and Korn, M. (1993). Single scattering theory versus numerical modelling in 2-D random media, *Geophys. J. Int.* **112**, 124–140.

*Sato, H. (1977). Energy propagation including scattering effect: Single isotropic scattering approximation, *J. Phys. Earth* **25**, 27–41.

Sato, H. (1979). Wave propagation in one-dimensional inhomogeneous elastic media, *J. Phys. Earth*, **27**, 455-466.

Sato, H. (1978). Mean free path of S-waves under the Kanto district of Japan, *J. Phys. Earth* **26**, 185–198.

*Sato, H. (1982). Amplitude attenuation of impulsive waves in random media based on travel time corrected mean wave formalism, *J. Acoust. Soc. Am.* **71**, 559–564.

*Sato, H. (1984). Attenuation and envelope formation of three-component seismograms of small local earthquakes in randomly inhomogeneous lithosphere, *J. Geophys. Res.* **89**, 1221–1241.

Sato, H. (1988). Temporal change in scattering and attenuation associated with the earthquake occurrence - A review of recent studies on coda waves, *Pure Appl. Geophys.* **126**, 465–497.

*Sato, H. (1989). Broadening of seismogram envelopes in the randomly inhomogeneous lithosphere based on the parabolic approximation: Southeastern Honshu, Japan, *J. Geophys. Res.* **94**, 17735–7747.

*Sato, H., and Fehler, M. (1998). "*Seismic Wave Propagation and Scattering in the Heterogeneous Earth*", AIP Preess/ Springer Verlag, New York.

*Sato, H., Nakahara, H., and Ohtake, M. (1997). Synthesis of scattered energy density for non-spherical radiation from a point shear dislocation source based on the radiative transfer theory, *Phys. Earth Planet. Inter*. **104,** 1-14.

Savage, J. C. (1966a). Attenuation of elastic waves in granular medium, *J. Geophys. Res.* **70**, 3935–3942.

Savage, J. C. (1966b). Thermoelastic attenuation of elastic waves by cracks, *J. Geophys. Res.* **71**, 3929–3938.

Scherbaum, F. and Wyss, M. (1990). Distribution of attenuation in the Kaoiki, Hawaii, source volume estimated by inversion of P wave spectra, *J. Geophys. Res.*, **95,** 12439-12448.

*Scherbaum, F., and Sato, H. (1991). Inversion of full seismogram envelopes based on the parabolic approximation: Estimation of randomness and attenuation in southeast Honshu, Japan, *J. Geophys. Res.* **96**, 2223–2232.

Shang, T., and Gao, H. (1988). Transportation theory of multiple scattering and its application to seismic coda waves of impulsive source, *Scientia Sinica* (series B, China) **31**, 1503–1514.

*Shapiro, S. A., and Kneib, G. (1993). Seismic attenuation by scattering: Theory and numerical results, *Geophys. J. Int.* **114**, 373–391.

Singh, S., and Herrmann, R. B. (1983). Regionalization of crustal coda Q in the continental United States, *J. Geophys. Res.* **88**, 527–538.

Spivack, M., and Uscinski, B. (1989). The split-step solution in random wave propagation, *J. Comp. Appl*i *Math.* **27**, 349-361.

Sreenivasiah, I., Ishimaru, A., and Hong, S. T. (1976). Two-frequency mutual coherence function and pulse propagation in a random medium: An analytic solution to the plane wave case, *Radio Sci.* **11**, 775–778.

*Stoffa, P., Fokkema, J., de Luna Friere, R., and Kessinger, W. (1990). Split-step Fourier migration, *Geophysics*, **55**, 410-421.

Tatarskii, V. L. (1971). The effects of the turbulent atmosphere on wave propagation (translated from Russian), Nat. Technical Information Service.

Taylor, S. R., Bonner, B. P., and Zandt, G. (1986). Attenuation and scattering of broadband P and S waves across North America, *J. Geophys. Res.*, **91**, 7309-7325.

Tittmann, B. R., Clark, V. A., and Richardson, J. M. (1980). Possible mechanism for seismic attenuation in rocks containing small amount of volatiles, *J. Geophys. Res.* **85**, 5199–5208.

*Tsujiura, M. (1978). Spectral analysis of the coda waves from local earthquakes, *Bull. Earthq. Inst. Univ. Tokyo* **53**, 1–48.

Tsumura, K. (1967). Determination of earthquake magnitude from duration of oscillation, *Zisin* (in Japanese) **20**, 30–40.

Varadan, V. K., Varadan, V. V., and Pao, Y. H. (1978). Multiple scattering of elastic waves by cylinders of arbitrary cross section. I. SH waves, *J. Acoust. Soc. Am.* **63**, 1310–1319.

Walsh, J. B. (1966). Seismic wave attenuation in rock due to friction, *J. Geophys. Res.* **71**, 2591–2599.

*Wu, R.-S. (1982). Attenuation of short period seismic waves due to scattering, *Geophys. Res. Lett.* **9**, 9–12.

*Wu, R. S. (1994).Wide-angle elastic wave one-way propagation in heterogeneous media and elastic wave complex-screen method, *J. Geophys. Res.*, **99**, 751-766.

*Wu, R.-S. (1985). Multiple scattering and energy transfer of seismic waves - separation of scattering effect from intrinsic attenuation - I. Theoretical modeling, *Geophys. J. R. Astron. Soc.* **82**, 57–80.

*Wu, R.-S. (1989). The perturbation method for elastic waves scattering, *Pure Applied Geophys*. **131**, 605-637.

Wu, R.-S., and Aki, K. (1985). Elastic wave scattering by random medium and the small-scale inhomogeneities in the lithosphere, *J. Geophys. Res.* **90**, 10261-10273.

*Wu, R.-S., and Flatté, S. M. (1990). Transmission fluctuations across an array and heterogeneities in the crust and upper mantle, *Pure Applied Geophys*. **132**, 175-196.

*Wu, R.-S., and Xie, X. B. (1991). Numerical tests of stochastic tomography, *Phys. Earth & Planet. Int*., **67**, 180-193.

Wu, R.-S., and Liu, X. P. (1995). Random layers found by joint coherence analyses of array data observed at NORSAR and SCSN, *EOS, Trans. Amer. Geophys. Union*, **76**, No. 46, F384.

Wu, R.-S., Xie, X. B., and Liu, X. P. (1994). Numerical simulations of joint coherence functions observed on seismic arrays and comparison with NORSAR data, *EOS, Trans. Amer. Geophys. Union*, **75**, No. 44, 478.

*Wu, R.-S., Jin, S., and Xie, X.-B. (2000). Seismic wave propagation and scattering in heterogeneous crustal waveguides using screen propagators: I SH waves, *Bull. Seismol. Soc. Am.*, in press.

*Yoshimoto, K., Sato, H., and Ohtake, M. (1993). Frequency-dependent attenuation of P and S waves in the Kanto area, Japan, based on the coda-normalization method, *Geophys. J. Int.* **114**, 165–174.

Yoshimoto, K., Sato, H., and Ohtake, M. (1997a). Three-component seismogram envelope synthesis in randomly inhomogeneous semi-infinite media based on the single scattering approximation, *Phys. Earth Planet. Inter*., **104,** 37-62.

*Yoshimoto, K., Sato, H., and Ohtake, M. (1997b). Short-wavelength crustal inhomogeneities in the Nikko area, central Japan, revealed from the three-component seismogram envelope analysis, *Phys. Earth Planet. Inter.* **104,** 63-74.

Yoshimoto, K., Sato, H., Iio, Y., Ito, H., Ohminato, T., and Ohtake, M. (1998). Frequency-dependent attenuation of high-frequency P and S waves in the upper crust in western Nagano, Japan, *Pure Appli. Geophys.*, **153**, 489-502.

*Zener, C. (1948). “Elasticity and Anelasticity of Metals”, University of Chicago Press, Chicago.

*Zeng, Y., Su, F., and Aki, K. (1991). Scattering wave energy propagation in a random isotropic scattering medium 1. Theory, *J. Geophys. Res.* **96**, 607–619.

*Zeng, Y., Aki, K. and Teng, T. L. (1993). Mapping of the high-frequency source radiation for the Loma Prieta earthquake, California, *J. Geophys. Res.* **98,** 11981–11993.

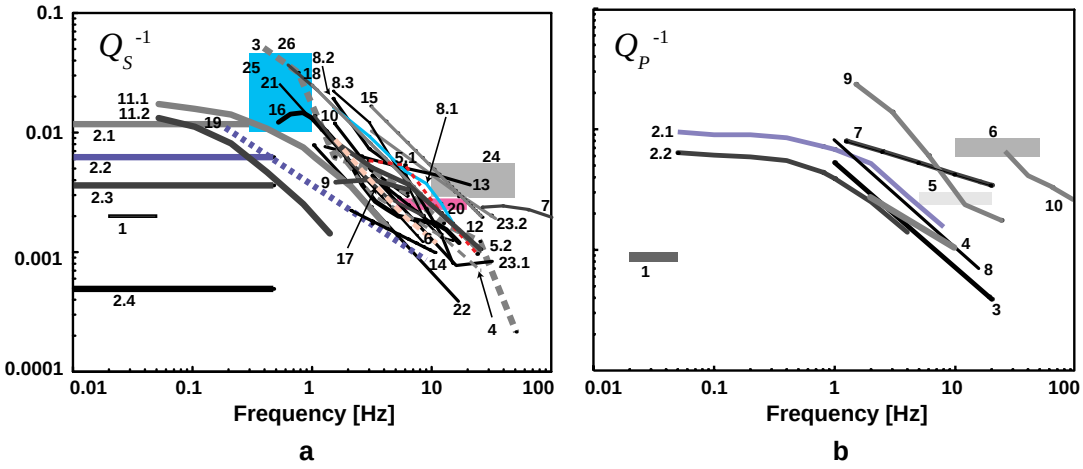
Q_S^{-1}
0.1
0.01
0.001
0.0001
0.01
0.1
1
10
100
Frequency [Hz]
a
Q_P^{-1}
0.01
0.1
1
10
100
Frequency [Hz]
b

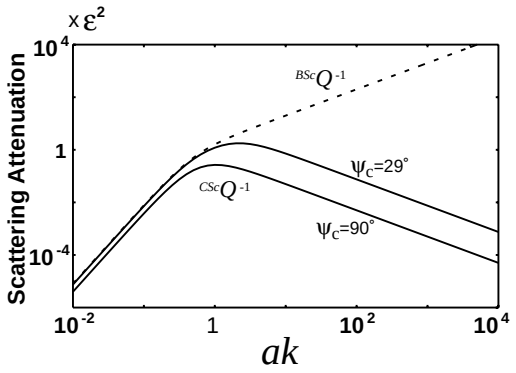
x ε²
Scattering Attenuation
10⁴
1
10⁻⁴
10⁻²
1
10²
10⁴
ak
BScQ⁻¹
CScQ⁻¹
ψc=29°
ψc=90°

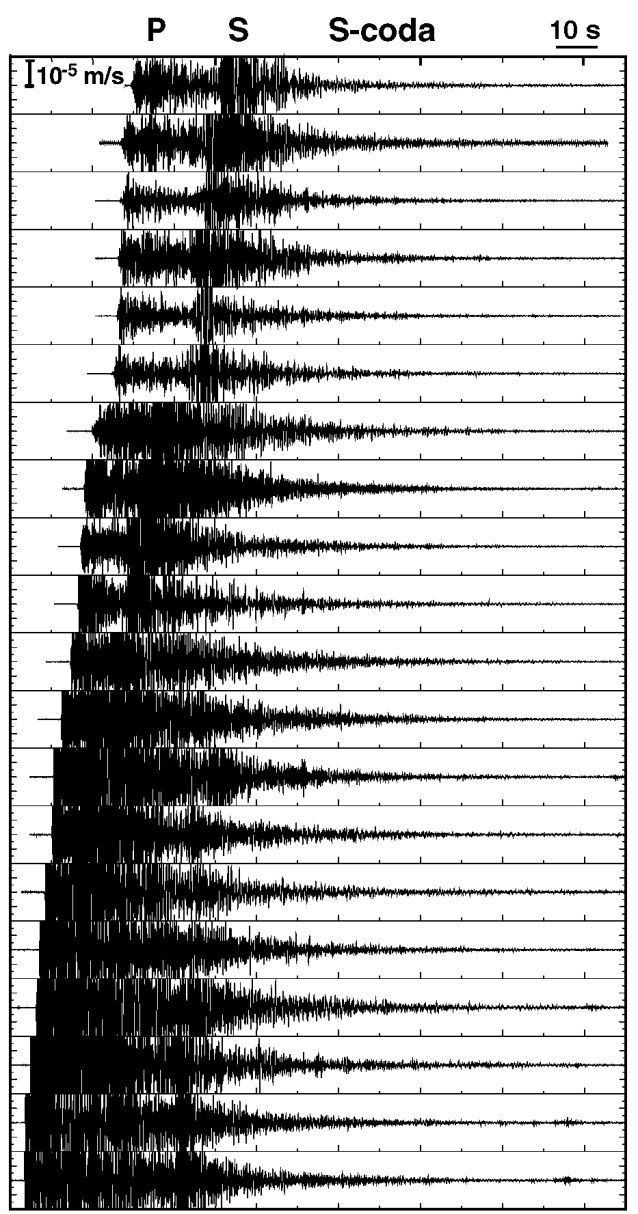
P
S
S-coda
10 s
10-5 m/s

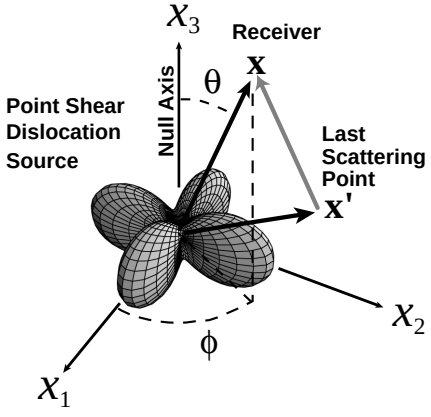
X_3
Receiver
x
θ
Null Axis
Point Shear
Dislocation
Source
Last
Scattering
Point
x'
X_2
ϕ
X_1

a

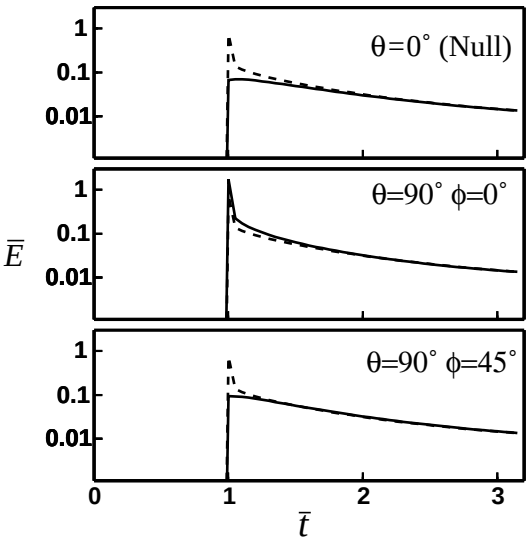
θ=0˚ (Null)
θ=90˚ ϕ=0˚
θ=90˚ ϕ=45˚
1
0.1
0.01
$\bar{E}$
0
1
2
3
$\bar{t}$

b

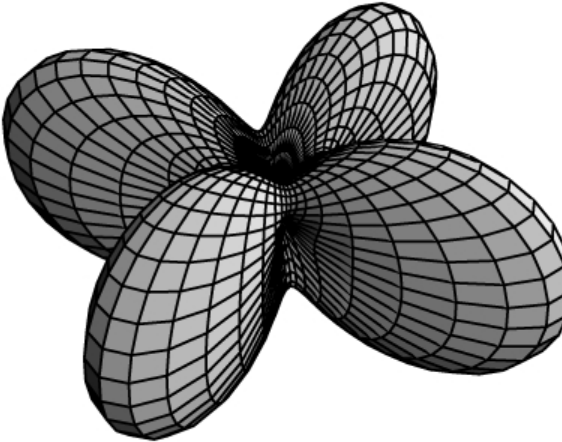

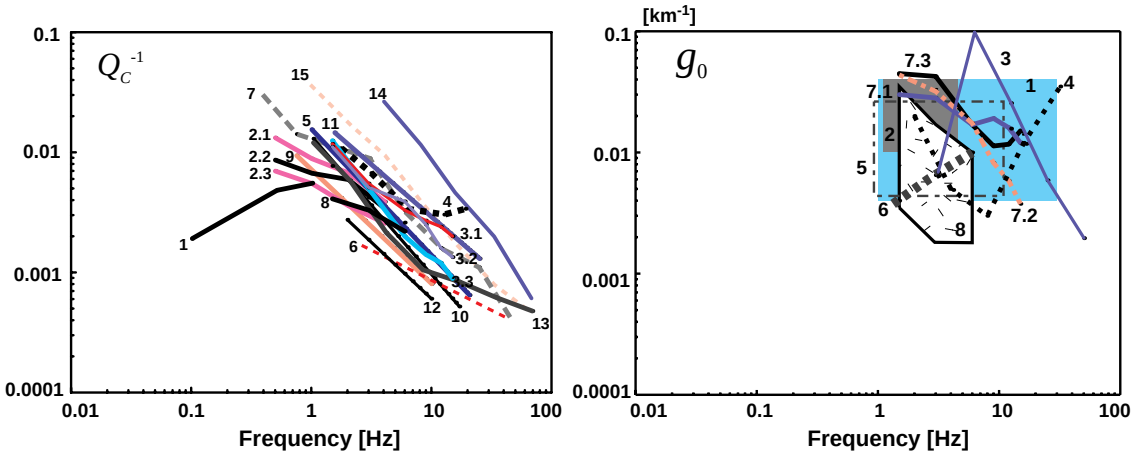
Q_C^{-1}
0.1
0.01
0.001
0.0001
0.01
0.1
1
10
100
Frequency [Hz]
a
[km^{-1}]
g_0
Frequency [Hz]
b

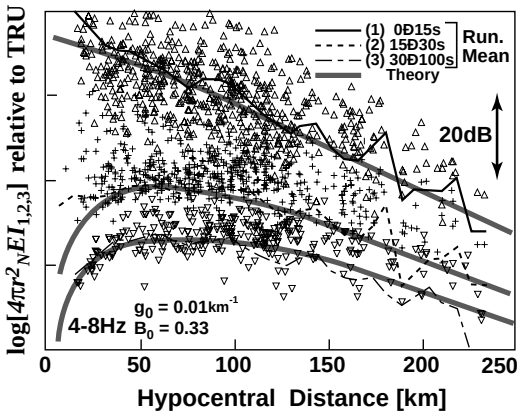
(1) 0Ð15s
(2) 15Ð30s
(3) 30Ð100s
Theory
Run. Mean
20dB
g_0 = 0.01km^{-1}
B_0 = 0.33
4-8Hz
log[4πr^2$_N$EI$_{1,2,3}$] relative to TRU
0
50
100
150
200
250
Hypocentral Distance [km]

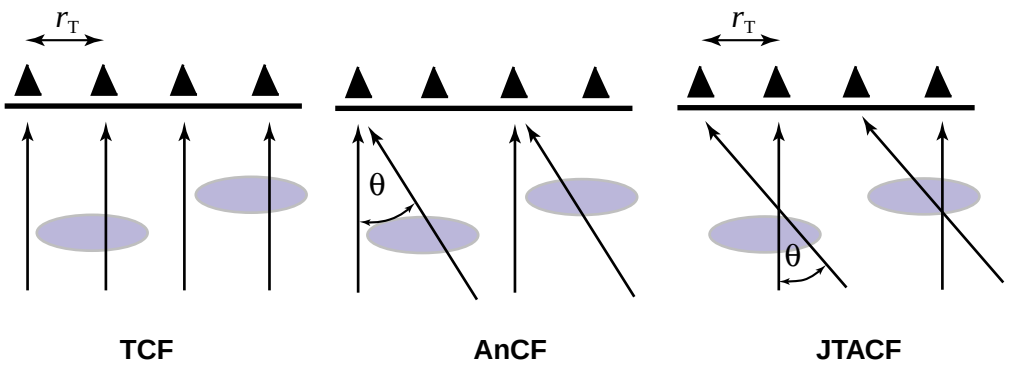
r_T
θ
r_T
θ
TCF
AnCF
JTACF

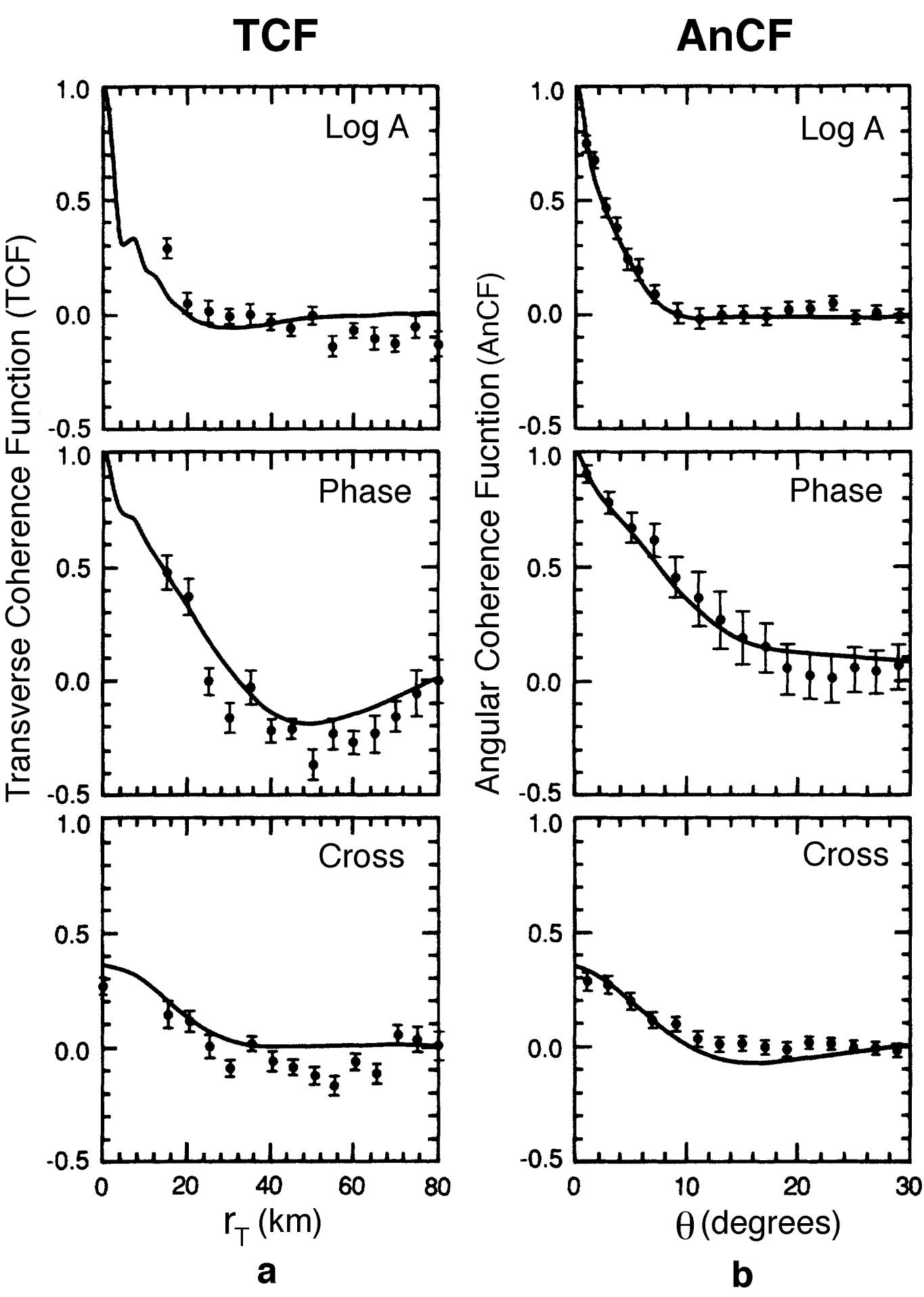
TCF
AnCF
Log A
Phase
Cross
Transverse Coherence Function (TCF)
Angular Coherence Fucntion (AnCF)
1.0
0.5
0.0
-0.5
0
20
40
60
80
10
30
r_T (km)
θ (degrees)
a
b